DOKUZ EYLUL UNIVERSITY
GRADUATE SCHOOL OF NATURAL AND APPLIED SCIENCES

PRODUCTION AND WEAR BEHAVIOUR OF MICRO-ARC COATED MAGNESIUM ALLOYS

by
Kadir Cihan TEKİN

January, 2010
İZMİR

PRODUCTION AND WEAR BEHAVIOUR OF MICRO-ARC COATED MAGNESIUM ALLOYS

A Thesis Submitted to the
Graduate School of Natural and Applied Sciences of Dokuz Eylul University
In Partial Fulfillment of the Requirements for the Degree of Master of Science
in Metallurgical and Materials Engineering, Metallurgical and Materials Program

by
Kadir Cihan TEKİN

January, 2010
İZMİR

M. Sc. THESIS EXAMINATION RESULT FORM

We have read the thesis entitled **"PRODUCTION AND WEAR BEHAVIOUR OF MICRO-ARC COATED MAGNESIUM ALLOYS"** completed by **KADİR CİHAN TEKİN** under revision of **ASSIS. PROF. DR. UĞUR MALAYOĞLU** and we certify that in our opinion it is fully adequate, in scope and in quality, as a thesis for the degree of Master of Science.

Assis. Prof. Dr. Uğur MALAYOĞLU

Supervisor

(Jury Member)

(Jury Member)

Prof. Dr. Cahit HELVACI

Director

Graduate School of Natural and Applied Science

ACKNOWLEDGEMENTS

I am grateful to many people who have been part of my life and who have made this dissertation possible. Many of those individuals are listed below, however, many more have played a role in my development as a person and a scientist.

First I would like to thank my advisor Assis. Prof. Dr. Uğur MALAYOĞLU for his guidance and support in this work. I am grateful for his patience and willingness to support my aspirations of obtaining an interdisciplinary degree and studying abroad, knowing the extra time and work that would be required of him.

I would like to extend my thanks to Assis. Prof. Dr. Ufuk MALAYOĞLU for his help, encouragement and valuable suggestions throughout this work.

I also would like to thank my all colleagues especially Emrah ÇAKMAK, Res. Assis. Esra DOKUMACI and Res. Assis. Osman ÇULHA for their cooperation, friendship and patience.

Finally, I would like to thank my all family for their support and persistence.

The present research was supported by (TUBITAK) with project code 107M495 named as; improving the wear and corrosion resistance of magnesium alloys by micro-arc oxidation method.

Kadir Cihan TEKİN

PRODUCTION AND WEAR BEHAVIOUR OF MICRO-ARC COATED MAGNESIUM ALLOYS

ABSTRACT

The objective of this study is to produce micro-arc oxide coatings on magnesium alloys and to investigate their structural, mechanical and tribological properties. Micro-Arc Oxidation (MAO) is an environmentally friendly and novel surface technology that forms a protective and well adhered ceramic coating on light metals such as magnesium, aluminium and titanium. In this study, AZ91D and AM60B magnesium alloys commonly used in automotive and aerospace industries were surface-treated using Keronite MAO equipment in an alkaline electrolyte with low concentrations of potassium hydroxide, potassium phosphate tribasic and sodium aluminate. Two different MAO coatings of 10 microns and 25 microns thickness were obtained. The microstructure and phase composition of MAO coatings were analysed using scanning electron microscopy (SEM) and X-ray diffraction (XRD) respectively. The scratch tests were carried out to determine the adhesion strength of the MAO coatings. The tribological behaviour of MAO coatings under dry sliding conditions against 100Cr6 steel ball was investigated using ball-on-plate test configuration. The results indicated that the adhesion strength of MAO coatings was improved with increasing coating thickness. The MAO coatings significantly enhanced the wear resistance of magnesium alloys with increasing coating thickness. For uncoated magnesium alloys, abrasive and adhesive wear mechanisms acted together during sliding motion while abrasive wear mechanism was predominant for MAO coatings.

Keywords: Micro-arc oxidation, wear, magnesium alloy, scratch, adhesion strength

MİKRO ARK KAPLANMIŞ MAGNEZYUM ALAŞIMLARININ ÜRETİLMESİ VE AŞINMA DAVRANIŞLARININ İNCELENMESİ

ÖZ

Bu çalışmanın amacı, magnezyum alaşımları üzerinde mikro-ark oksit kaplamalar üretmek ve kaplamaların yapısal, mekaniksel ve tribolojik özelliklerini incelemektir. Mikro-Ark Oksitleme (MAO), magnezyum, aluminyum ve titanyum vb. hafif metallerin üzerinde koruyucu ve yüzeye iyi tutunan seramik kaplama oluşturan, çevreye karşı duyarlı ve yeni bir yüzey teknolojisidir. Bu çalışmada, otomotiv ve havacılık sanayinde çoğunlukla kullanılan AZ91D ve AM60B magnezyum alaşımları, Keronite MAO donanımı kullanılarak düşük konsantrasyonlarda potasyum hidroksit, potasyum fosfat tribazik ve sodyum aluminat ihtiva eden alkali elektrolit içerisinde yüzey işlemine tabi tutulmuştur. 10 mikron ve 25 mikron kalınlığında iki ayrı kaplama elde edilmiştir. Kaplamaların mikroyapısı ve faz bileşenleri sırasıyla taramalı elektron mikroskopisi (SEM) ve X-ışını difraksiyonu (XRD) kullanılarak analiz edilmiştir. Kaplamaların yapışma mukavemetinin belirlenmesi amacıyla kazıma testleri yapılmıştır. MAO kaplamaların kuru ortamdaki tribolojik davranışı, 100Cr6 çelik bilya karşı elemanı kullanılarak bilya-levha aşınma çifti test modunda incelenmiştir. Test sonuçlarında, MAO kaplamaların yapışma mukavemetinin artan kaplama kalınlığı ile arttığı gözlenmiştir. MAO kaplamalar artan kaplama kalınlığıyla birlikte magnezyum alaşımlarının aşınma direncini önemli derecede arttırmıştır. Aşınma deneyleri esnasında magnezyum alaşımları için abraziv ve adheziv aşınma mekanizmaları birlikte rol alırken, MAO kaplamalar için abraziv aşınma mekanizması daha etkin olmuştur.

Anahtar kelimeler: Mikro-ark oksitleme, aşınma, magnezyum alaşımı, kazıma, yapışma mukavemeti

CONTENTS

Page

M. Sc. THESIS EXAMINATION RESULT FORM ii
ACKNOWLEDGEMENTS iii
ABSTRACT iv
ÖZ v

CHAPTER ONE – INTRODUCTION 1

CHAPTER TWO – SURFACE PROTECTION OF MAGNESIUM ALLOYS .. 5

2.1 Surface Protection Methods 5
2.1.1 Anodising 6
2.1.2 Gas-Phase Deposition Processes 8
2.1.3 Organic-Polymer Coatings 10
2.1.4 Micro-Arc Oxidation (MAO) 12

CHAPTER THREE – MICRO-ARC OXIDATION 13

3.1 Background 13
3.2 Development of MAO Process 13
3.3 Processing 16
3.3.1 MAO Equipment 16
3.4 Coating Formation 18
3.4.1 Electrochemical Characteristics 18
3.4.2 Discharge Characteristics 19
3.4.3 Electrochemistry of MAO 21
3.4.4 Plasma discharge models and plasma chemistry 25
3.5 Tribological Properties of MAO Coatings 29

3.6 Commercialisation of MAO Process 31
3.6.1 Magoxid-Coat Process 31
3.6.2 Tagnite Process 32
3.6.3 Keronite Process 33

CHAPTER FOUR – EXPERIMENTAL STUDIES 34

4.1 Purpose 34
4.2 Materials 34
4.3 MAO Process 35
4.3.1 Substrate Preparation 35
4.3.2 Electrolyte Preparation 36
4.3.3 Preparation of MAO Coatings 37
4.4 Coating Thickness Measurement 38
4.5 Microstructural Investigation 38
4.5.1 SEM Observation 38
4.5.2 X-ray Diffraction 39
4.5.3 Surface profilometry and roughness measurement 39
4.6 Hardness measurement 40
4.7 Scratch Test 40
4.8 Wear Test 41

CHAPTER FIVE – RESULTS AND DISCUSSION 43

5.1 Substrate Characterisation 43
5.2 Characterisation of MAO Coatings 45
5.2.1 Surface Morphology and Structure of MAO Coatings 45
5.2.2 X-ray Diffraction 49
5.2.3 Surface profilometry and roughness measurement 50
5.3 Mechanical Properties 52
5.3.1 Hardness Measurement and Scratch Test 52

5.4 Tribological Behaviour 54
5.4.1 Dry Sliding Wear Test 54

CHAPTER SIX- CONCLUSION 61

6.1 General Results 61
6.2 Future Plans 62

REFERENCES 63

CHAPTER ONE
INTRODUCTION

Magnesium based materials are commonly used in automotive and aerospace industries due to providing reduced mass which decreases the fuel consumption while offering desired physical properties. The main applications of magnesium alloys in automotive industry include seat frames, gearbox housing, pistons, steering wheels, rims and dashboards etc. However the problem with the isolation of magnesium was associated with its reactivity, which has haunted all those interested in using magnesium as components. Also if we consider other properties such as elastic rigidity and hardness we find that these are significantly lower than those of other metals. In this case different surface treatments including electrochemical plating (Das, 2003) and (Fontana, 1996), conversion coating (Udhayan, & Bhatt, 1996), (Umehara, Takayaand, & Terauchi, 2003) and (Gonzalez-Nunez, Nunez-Lopez, Skeldon, et al., 1995), PVD (Hollstein, Wiedemann, & Scholz, 2003), anodising and organic coating have been developed in order to compensate poor wear and corrosion resistances of magnesium alloys. Each of these techniques has its own merits and limitations. The chemical conversion and anodising are the most popular methods which usually offer a relatively simple and cost-effective way; however, the coatings are rather thin, porous and cannot allow sufficient hardness values to be achieved for effective wear protection of magnesium alloys in aggressive service conditions. Also they use acidic solutions such as phosphoric acid, chromate or chromic acid, and/or hydrofluoric acid. Due to environmental and carcinogenic concerns hexavalent chrome and fluorides are currently being phased out by Occupational Safety and Health Administration OSHA.

Recently, introduction of advanced coatings with exceptional anti-corrosion and anti-wear performance provided further possibilities in improving performance of magnesium alloys (Gray, & Luan, 2002). Miao, Cui, & Pan (2007) found that CrN–TiN multilayer coatings on AZ91D magnesium alloy could effectively improve the performance of wear resistance and corrosion resistance. Combined thermal

spray/MoS_2 composite coatings on magnesium alloy were obtained by Gadow, & Scherer (2002)and the concept of combined coatings can be used to greatly improve the friction and wear properties under dry sliding conditions. Yamauchi et al. (2005) reported that diamond-like carbon (DLC) coatings on magnesium alloy show better tribological performance and corrosion resistance. Hoche, Scheerer, Probst, Broszeit, & Berger (2003) and Hoche, Schroeder, Scheerer, Broszeit, & Berger (2002) reported the wear behaviour of the PVD-CrN coatings on magnesium die-cast alloy AZ91 at temperature from room temperature to 250 ^{o}C. However, in recent years, the surface treatment industry is focused on the replacement of chromate-based coatings with other environmentally friendly alternatives including an advanced surface technology named micro-arc oxidation (MAO). This method which refers to the same process as plasma electrolytic oxidation (PEO) and anodic spark deposition (ASD) does not involve any hazardous electrolyte components such as hexavalent-Cr or heavy metals.

MAO process is based on plasma-assisted anodic oxidation which forms protective and well adhered ceramic coatings on valve metals such as magnesium, aluminium and titanium etc. (Yerokhin, Nie, Leyland, Matthews, & Dowey, 1999). MAO differs from conventional anodising with respect to its high operating voltages which cause dielectric breakdown of the passive film formed on the surface of metal substrate. This causes micro-arcs to occur and results in more crystalline/ceramic type coatings. The coatings produced via MAO process provide a continuous barrier layer with high hardness as compared to anodising.

In the last decade, MAO has become a well-developed technology, with commercial variants such as those produced by Keronite^{TM} (Keronite Coating), Aalberts Industries Material Technologies Group (MAGOXID-COAT$^{®}$) and Technology Applications Group (Tagnite Coating System) achieving wide acceptance in industry. Their development, however, has been largely empirical and understanding of the coatings remains at a very early stage.

Many factors affecting the MAO process such as current density, voltage, electrolyte additives, pre- and post-treatments were investigated (Jin, et al., 2006), (Liang, et al., 2007), (Duan, et al., 2007), (Liang, et al., 2005) (Cai, et al., 2006), (Ximei, et al., 2008), (Hutchins, Shashkov, et al., 2004) and (Hutchins, Shrestha, et al., 2004). The growth mechanism of MAO coatings on metallic materials has also been discussed (Rakoch, Khokhlov, Bautin, Lebedeva, Magurova, & Bardin, 2006). Variations in electrolyte compositions and the power supply cause the difference in the MAO process characteristics such as breakdown voltage and final voltage thus the properties of MAO coating e.g. thickness, roughness, porosity, inward and outward growth, phase composition, hardness, and coating formation rate are changed. Both coatings produced in silicate and phosphate electrolytes provide effective protection for the wear resistance compared with the uncoated magnesium alloy. The electrolyte constituents exert a decisive influence on phase composition of the MAO films. The MAO coating formed in silicate electrolyte was reported to have compact and uniform coating layer while the coating formed in phosphate electrolyte had a relatively porous structure.

In the present work, two different MAO coatings of 10 μm and 25 μm thickness on AZ91D and AM60B magnesium alloys were obtained using MAO process. Cross-sections and surface morphologies of MAO coatings were evaluated using SEM (Scanning Electron Microscopy). The structural investigation allows structure-property relationships to be established, and also helps to elucidate the mechanism of coating formation. XRD (X-ray Diffraction) was used in order to determine the phase compositions of coatings. The adhesion strength of MAO coatings was obtained by scratch test. Adhesion strength is a significant factor in determining the wear resistance of coatings. Tribological behaviour of MAO coatings under dry sliding conditions against 100Cr6 steel ball was investigated using ball-on-plate test configuration.

This thesis contains six chapters. Chapter 1 gives a preface to micro-arc oxidation, including an overview, description and development of process. Chapter 2 provides introductory information about the surface modification techniques that have been

used in order to improve the poor wear resistance of magnesium and its alloys. The advantages and limitations of these techniques have also been discussed. Chapter 3 gives detailed information about the historical background of micro-arc oxidation and the mechanism of coating formation. Moreover, Chapter 3 provides useful information about the tribological properties of the coatings that are produced using this process. Chapter 4 introduces the experimental techniques used in the present study. These include specimen preparation, characterisation methods such as scanning electron microscopy (SEM), X-ray diffraction (XRD) and tribological tests. The results and interpretations of experimental studies which help to clarify tribological behaviour of MAO coatings were given in Chapter 5. Chapter 6 is the final chapter of this study where concludes arrived judgements with respect to logical thinking.

CHAPTER TWO
SURFACE PROTECTION OF MAGNESIUM ALLOYS

2.1 Surface Protection Methods

Magnesium alloys offer new ways in light weight engineering due to their low specific weight and their high strength to weight ratio. But, their application is limited up to now to the static component field because of the bad wear properties of magnesium alloys. However, a considerably higher potential for the lasting fuel and emission reduction could be the application of magnesium alloys for moving parts by ensuring a sufficient wear resistance. Therefore an effective and appropriate coating technology has to be adapted to enable a successful implementation of magnesium alloys under tribological load and in corrosive environment.

There are a number of surface treatments for magnesium have been used or proposed over the years, and new ideas continue to be disclosed. These include conversion coatings, such as chromates (now being phased out on health grounds), phosphates (where certain operational problems can occur), processes based on fluoride treatment (taking advantage of the relatively insoluble magnesium fluoride), and a range of mixed inorganic plus organic coatings and also use of electroless nickel or plasma or thermally-sprayed coatings. Most of these treatments have significant drawbacks. In the case of plasma or thermally sprayed coatings, for example, adhesion can be a problem, unless the substrate surface is significantly heated, which is not always possible. In some cases, such coatings offer predominantly corrosion protection. In other cases, they are designed to improve tribological behaviour - magnesium alloys have high wear rates in their untreated state and are subject to galling.

The following text addresses the surface technologies applied to magnesium alloys in order to improve their wear resistance. The list does not include all methods but the most used surface treatments are mentioned.

2.1.1 Anodising

Anodising is the most widely used commercial coating technology for magnesium and its alloys. This process is technologically more complex than electroplating or conversion coating process. It does involve more capital investment due to the need for cooling systems and high power consumption. Anodising is an electrolytic process for producing a thick, stable oxide film on metals and alloys. These films may be used to improve paint adhesion to the metal, as a key for dying or as a passivation treatment. The stages for processing include; (1) mechanical pre-treatment, (2) degreasing, cleaning, and pickling, (3) electro brightening or polishing, (4) anodising using AC or DC current, (5) dying or post-treatment and (6) sealing (Gray, & Luan, 2002).

The films have a thin barrier layer at the metal-coating interface followed by a layer that has a cellular structure. Each cell contains a pore whose size is determined by the type of electrolyte and its concentration, temperature, current density and applied voltage. Their size and density determine the extent and quality of sealing of the anodised film (Mittal, 1995). Colouring of anodised films can be achieved by absorbing organic dyes or inorganic pigments into the film immediately after anodising, by a second-step electrolytic deposition of inorganic metal oxides and hydroxides into the pores of the film or by a process called integral colour anodising (Gray, & Luan, 2002).

Sealing of the anodised film is necessary in order to achieve an abrasion and corrosion resistant film. This can be accomplished by boiling in hot water, steam treatment, dichromate sealing and lacquer sealing (Gray, & Luan, 2002). One of the main challenges for producing adherent, wear resistant, anodic coatings on magnesium results from the electrochemical inhomogeneity due to the phase separation in the alloy. Another disadvantage of this technique is that the fatigue strength of the base metal can be affected by localized heating at the surface during the treatment.

DOW 17 process Chemical treatment no. 17, developed by Dow Chemicals, can be applied to all forms and alloys of magnesium (Hillis, 1994). The anodising bath employed in this treatment is a strongly alkaline bath consisting of an alkali metal hydroxide and a fluoride or iron salt or a mixture of the two. This process produces a two-phase, two-layer coating. The first layer is deposited at a lower voltage and results in a thin, approximately 5 μm, light green coating. The over layer is formed at a higher voltage. It is a thick dark green, 30 μm, layer that has good abrasion resistance, paint base properties and corrosion resistance (Hillis, 1994).

HAE process named after its founder, H. A. Evangelides. This treatment can be applied to all magnesium alloys including the rare-earth magnesium alloys (Evangelides, 1951). The HAE bath is a strongly alkaline and oxidising solution, consisting of potassium-hydroxide-aluminate-fluoride-manganate and tribasic sodium phosphate (Anonymous, 1957). The treatment produces a two phase coating as in the DOW 17 process. At a lower voltage a 5 μm thick, light tan sub coating is produced. At a higher voltage a dark brown, thicker (30 μm) film is produced. The dark brown coating is hard with good abrasion resistance but it can adversely affect the fatigue strength of the underlying magnesium, particularly if it is applied on thin magnesium sections (Gray, & Luan, 2002). Upon sealing the HAE treatment provides good wear resistance.

ANOMAG process is a proprietary treatment invented by Magnesium Technology Licensing Ltd. The anodising bath for this process consists of an aqueous solution of ammonia and sodium ammonium hydrogen phosphate (Barton, 1998). The coating produced is a mixed $MgO–Mg(OH)_2$ system with the possibility of additional compounds such as $Mg_3(PO_4)_2$ depending on any additives present in the bath. Due to the presence of ammonia in the system, spark formation is repressed, which eliminates the need for cooling equipment. The coatings produced are semi-transparent to pearl coloured depending on the presence and concentration of certain additives such as fluoride and aluminate. Coatings applied to magnesium alloy substrates may vary in thickness from as little as 5 microns to a maximum of around 25 microns.

2.1.2 Gas-Phase Deposition Processes

Protective coatings can also be produced from the gas phase. These are typically metallic coatings but can include ceramic coatings, diamond like coatings and organic coatings such as thermal spray polymer coatings.

In thermal spray coating process the coating material which can be metal, ceramic, cermet or polymeric is fed to a torch or gun where it is heated to above or near its melting point. The resulting droplets are accelerated in a gas stream onto the substrate and the droplets flow into thin lamellar particles and adhere to the surface (Unger, 1987). There are a number of coating techniques including flame spraying, wire spraying, detonation gun deposition, plasma spray and high velocity oxyfuel.

It is reported that the arc sprayed Al-Si coatings are able to improve the wear resistance of magnesium alloys to an extent of at least 100% and even to offer an effective corrosion protection when sealed. By means of HVOF process it is also possible to produce very hard coatings, e.g. NiCr, NiCr-Cr_3C_2, able to improve the wear resistance of magnesium alloys in a significant manner (Lugscheider, & et al., 2004).

Some of the advantages of this technique include the ability to create a coating of virtually any material that melts without decomposing, minimal substrate heating during deposition and the ability to strip and recoat worn or damaged coatings without changing the properties or dimensions of the part (Unger, 1987).

One major disadvantage is that the process is line of sight and small deep cavities cannot be coated, especially if the surface lies parallel to the spray direction. Due to their inherent porosity and mechanical finishing these coatings also require sealing to obtain a smooth finishing. One final disadvantage of this technique is the health and safety issues generated by the production of dust, fumes, noise and light radiation during treatment.

Chemical vapour deposition (CVD) can be defined as the deposition of a solid on a heated surface via a chemical reaction from the gas phase. Advantages of this technique include deposition of refractory materials well below their melting points, achievement of near theoretical density, control over grain size, processing at atmospheric pressure and good adhesion (Bunshah, 2001). However, CVD is limited to substrates that are thermally stable at > 600 °C. Efforts are underway to reduce the high temperature requirements and plasma and organometallic CVD processes offset this problem somewhat. A further disadvantage of this process is high-energy cost due to the need for high deposition temperatures and sometimes low efficiency of the process.

Diamond like carbon films (DLC) can be produced using a number of different processes such as physical vapour deposition (PVD), CVD and ion implantation. These coatings are desirable for many applications due to their high hardness, low friction coefficient, electrical insulation, thermal conductivity and inertness. Yamauchi et al. (2005) reported that DLC films were deposited on the AZ31B magnesium alloy substrate by the plasma CVD method using radio frequency. The DLC coating was confirmed to be effective in decreasing the friction coefficient and improving the corrosion resistance in 3 wt. % NaCl and 0.05 N NaOH solutions.

Physical vapour deposition processes involves the deposition of atoms or molecules from the vapour phase onto a substrate. There are a few challenges to overcome in the PVD coating of magnesium substrates. The deposition temperature must be below the temperature stability of magnesium alloys and good adhesion must be obtained despite this low temperature. Modern developments use Al, Cr, Mn, V, and Ti layer technologies (Kainer, 1971). Since Cr has a good connection to the substrate, it is used as a bonding agent on AM50 and AZ91. The wear resistance of the Cr layer is further improved by using N_2 as the process gas, which results in a hard CrN coating (Kainer, 1971).

Extensive research of the authors in deposition of reliable PVD hard coatings on magnesium alloys showed comparable wear results in a certain parameter field in

comparison to PVD coated titanium- and iron-based alloys (Hoche, Blawert, Broszeit, & Berger,2004).

Hoche et al. (2002) investigated the wear behaviour of PVD-CrN coatings on magnesium die-cast alloy AZ91. It is found that at higher loads and temperatures the coatings failure and cannot satisfy the desired wear protection. This is attributed to the deformation of substrate due to its unsatisfactory load carrying capacity. So there is a need to improve the surface hardness to prevent plastic deformation. It may be useful to deposit a ductile interlayer between the CrN and the AZ91, to absorb coating cracks and inhibit coating detachment.

2.1.3 Organic-Polymer Coatings

Organic finishing is typically used in the final stages of a coating process. These coatings can be applied to enhance corrosion resistance, abrasion and wear properties, or for decorative purpose. An appropriate pre-treatment process is required in order to produce coatings with desired adhesion and appearance (Gray, & Luan, 2002). Many coating processes can be applied to magnesium and its alloys, including painting, powder coating, e-coat processing. But their thicknesses might be limited.

One of the most important steps in painting of magnesium is choosing an appropriate primer. Primers for magnesium should be alkali-resistant and based on resins such as polyvinyl butyral, acrylic, polyurethane, vinyl epoxy and baked phenolic (Hillis, 1994). The addition of zinc chromate or titanium dioxide pigments is commonly used for corrosion prevention.

Powder coating is a process in which a pigmented resinous coating powder is applied to the substrate and then heated to fuse the polymer together in a uniform, pinhole-free film. Powder coatings can be applied in a number of ways including electrostatic powder spraying, fluidized bed or flame spraying of thermoplastic powders. Powder coating is an excellent alternative to traditional painting processes

since it is not detrimental to the environment and uniform thick coatings can be obtained in a single operation even on rough surfaces or edges. There is also little loss of coating material during application and even basic resins that are not readily soluble in organic solvents can be applied. However, there are a few inherent disadvantages of this technique;

1. The powder must be maintained in a very dry, pulverized form.
2. Thin coatings are difficult to obtain.
3. Colour matching and colour uniformity can be difficult to significant amount of oxygen and chrome on the surface maintain.
4. Coating in recessed areas can be difficult.
5. High temperatures required for curing may be unacceptable for some substrates (Gray, & Luan, 2002).

E-coat or cathodic epoxy electro-coat is a process for painting metal surfaces by charging the metal part negative and submerging it in a tank that contains positively charged paint. The paint is attracted to the metal to form a uniform coating that is subsequently cured by baking (Gray, & Luan, 2002). However, the coating is quite thin therefore it should be combined with a thicker top coat. This process eliminates the environmental hazard posed by using traditional chromate containing conversion or anodised coatings.

If the polymeric coatings are applied to substrate metal without any base coating or pre-treatment, they usually exhibit unsatisfactory hardness and adhesion to the substrate. So they can be produced as multilayer coatings to increase adhesion strength and load carrying capacity. Even if polymeric coatings have lower hardness compared to ceramic ones, they can be used to improve dry lubrication properties of magnesium in wear applications.

2.1.4 Micro-Arc Oxidation (MAO)

As mentioned above, there are many techniques have been developed for wear protection of magnesium alloys. However, it appears that their disadvantages outweigh than their advantages. Therefore, the surface engineering industry needs to new processes which are environmentally friendly and have small capital investment. Micro-arc oxidation (MAO), also called plasma electrolytic oxidation (PEO), anodic spark deposition (ASD) or anodic plasma oxidation (ANOF), is a promising surface treatment which is based on plasma assisted anodic oxidation process. It is generally used in order to improve the wear and corrosion resistance of lightweight metals. In this technique high voltages are used to form discharges near the surface of a workpiece which is used as the anode immersed in a slightly alkaline electrolyte. Discharging melts the substrate metal and subsequently the released molten metal solidifies forming a ceramic-like oxide coating on the surface. The ceramic layer is sintered during the processing due to high local temperatures and adhered to the substrate very firmly. Thus the increasing adhesion and hardness of oxide coating provide excellent wear resistance.

The historical background, development, principles, tribological behaviour and applications of MAO will be discussed in the next Chapter in depth.

CHAPTER THREE
MICRO-ARC OXIDATION

3.1 Background

Microarc Oxidation (MAO) is a promising and environmentally friendly coating method which is based on plasma-assisted anodic oxidation that forms a protective and well adhered ceramic coating on valve metals such as magnesium, aluminium and titanium (Yerokhin, & et al. 1999). MAO is a generic term which is used to describe a variety of high voltage electrochemical processes, which feature plasma-discharge phenomena occurring at an electrode-electrolyte interface. The plasma discharges occur at the metal/electrolyte interface when the applied voltage exceeds a certain critical breakdown value (typically several hundreds of Volts). Discharge phenomena have been observed in both positive and negative biasing of a metal electrode and, depending on the electrode-electrolyte combination and polarisation parameters, can vary widely in appearance: from a steady uniform glow surrounding the electrode to discrete short-lived microdischarges moving rapidly across its surface.

3.2 Development of MAO Process

The first recorded observations of discharges during an electrolysis process were made in 1844 by Fizeau and Foucault. They noted luminescence on electrode surfaces during the electrolysis of water. It is likely that this was the result of arc discharges in hydrogen bubbles. In 1878, Sluginov became the first person to note a similar discharge phenomenon during the anodising of metals. Despite the phenomenon having been observed at the very outset of research into electrolysis, no attempts were made to control or harness the effects. Indeed, the first comprehensive study of “sparking phenomena” during aluminium anodising, published by Gunterschultze and Betz in 1932, concluded that such discharges were detrimental to the properties of coatings and should be avoided. They observed that the material

underwent deposition of the electrolyte during the dielectric breakdown of an insulating film growing on the anode. This dielectric breakdown causes sparks which appear and disappear while being distributed over the entire surface of the anode, giving the effect of movement. The first practical applications of anodic spark deposition (ASD) were their use as anticorrosion coatings on magnesium alloys, dating from 1936, and these were included in a military specification in 1963 (Beauvir, 2004).

Despite the concerns of Gunterschultze and Betz, sparking during anodising soon became an accepted part of the "spark anodising" of magnesium (Evangelides, 1951), (Huber, 1953) and a patent for the electrolytic coating of magnesium and its alloys was issued to Evangelides, (1955). His HAE process, and the similar DOW 17 process, has since become two of the most favoured anodizing processes for magnesium. The intensive sparking was found to result in the formation of thick deposits with a partially vitrified structure, which resembled sintered ceramics. These films were, however, very porous, containing many spherical gas bubbles, to the detriment of their mechanical properties.

Since then, the main research efforts have been pursued by Gruss, McNeill and coworkers at the Frankford Arsenal in Philadelphia, and by Brown, Wirtz, Kriven and coworkers at the University of Illinois in Urbana-Champaign (Beauvir, 2004).

The synthesis of cadmium niobate by McNeill & Nordbloom, (1958) is another early example of the application of micro arc oxidation. They used a spark discharge to synthesize $Cd_2Nb_2O_7$ on a cadmium anode in an aqueous solution of potassium niobate. It had thus been noted that constituents of the electrolyte (other than oxygen) could be incorporated into the oxide film to modify its properties and this was soon applied to the spark anodising of magnesium. Films formed in aluminate and silicate solutions were found to consist of a mixture of crystalline MgO and either $MgAl_2O_4$ or Mg_2SiO_4 respectively. McNeill & Gruss, (1966) subsequently filed a wide-ranging patent for "anodic spark reaction processes and reactions", granted in 1966. This

describes the application of hard alumina, silicate or tungsten trioxide-based coatings to a wide range of metals, including iron and gold.

At the same time, research was carried out in East Germany, mainly by Krysmann, Kurze, Dittrich and coworkers. The German process is called “anodic oxidation by spark discharges” (the German acronym for which is ANOF [Anodische Oxidation an Funkenanladung]). The reports of this work in the international literature make reference to patents in the German language. It is clear that this research has made significant progress, yet it remains, despite everything, superficial and the compounds of the coating formed have not been clearly identified (only the α-Al_2O_3 and γ-$Al_2O_3(OH)$ (bohemite) have been identified by X-ray diffraction) (Beauvir, 2004).

Significant developments and improvements to the process were subsequently undertaken in the USSR during the 1970s and 1980s. Researchers were particularly interested in the potential benefits of MAO discharges as an enhancement of the conventional anodising of aluminium. They noted that, under certain conditions, discharges provided a mechanism for faster oxide growth, and that the resulting oxide films were very hard. Gradovsky filed the first USSR patent for a “method of coating metals using anodic discharges” in 1974. Meanwhile, Van, Brown, & Wirtz, (1977) from the University of Illinois, published the first study of the “Mechanism of Anodic Spark Deposition”.

One process, patented in 1974, was developed in order to compete with coatings on aluminium for architectural purposes. The method allows the aluminium substrate to act as an anode in a potassium silicate solution so that an aluminosilicate coating of olive-grey colour is applied by using a 400 V half-wave rectified DC current. The process takes place by dielectric breakdown of the barrier layer, causing sparks or scintillations visible on the anodic substrate, while Bakovets, Dolgoveseva and Nikoforova postulate three parallel mechanisms during formation of the film, namely electrochemical, plasma oxidation and chemical oxidation mechanisms.

In 1982, Markov et al filed a patent for “AC and pulsed bipolar processes for the production of hard oxide ceramic coatings on Al”, heralding the start of Russian research into the process as a competitor for hard anodising. This was a major milestone in the development of this process; its potential benefits had finally been recognised, and commercial interest increased markedly. Further work by Tchernenko and Snezhko between 1980 and 1995 developed the technology of anodic spark deposition to the point where, in 2000, commercial equipment was available from such sources as *Keronite*™ in the USA and UK, and *Carl Zeiss* in Germany.

3.3 Processing

Since micro-arc oxidation is based on conventional anodizing, any of valve metals whose oxides have semiconducting property can be used to form thick oxide coatings on their surface.

Magnesium cannot be anodized in the same way as aluminium. In the case of Mg, the porous oxide seen on anodized aluminium does not form. These pores are essential for ion transport, which is part of the film growth process, and in their absence maximum film thickness under classical anodizing conditions is limited. In addition, the oxide film formed over anodized magnesium is much more highly stressed than its aluminium analog. In consequence, it is brittle and prone to fracture during or after anodizing.

3.3.1 MAO Equipment

The equipment used for MAO is similar to that used for conventional anodising, but more complex, primarily due to the need for higher potentials and controlled pulses of current.

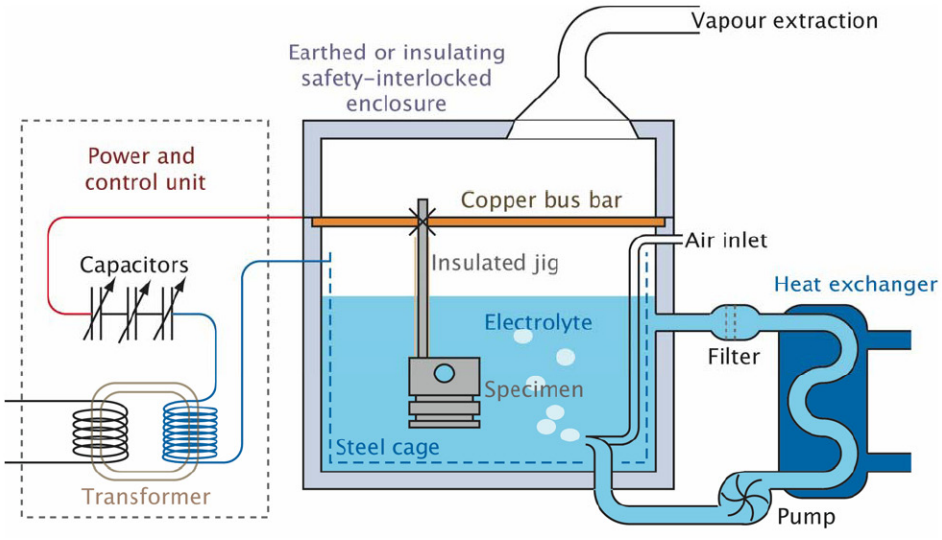


Figure 3.1 Schematic of typical MAO equipment, as described in the following text.

A typical equipment for MAO processing consists of an electrolyser and a high power electrical source (Figure 3.1). The electrolyser is commonly an insulated bath, made of a polymer-based material, in which the stainless steel counter electrodes are placed. The electrolyser incorporates a pump for re-circulating the electrolyte, a heat-exchanger for cooling the electrolyte and a gas exhausting arrangements, as well as electrical interlocks. Cooling of the electrolyte is necessary to prolong its useful lifetime. If it is allowed to heat up beyond 30 ºC, the coating process can be faster but the electrolyte is depleted of active ingredients much more rapidly. The component to be coated is cleaned and degreased. It is then electrically connected via an insulated aluminium or titanium jigging arrangement to the copper bus bar, and thus becomes the working electrode.

Various types of power source can be used to bring about plasma electrolysis (Yerokhin, & et al., 1999). According to the applied electrical regime they can be classified into the following groups: DC, pulsed bipolar DC and AC sources. Because of difficulties in regulating the surface discharge characteristics DC power sources are used only for simple-shape components and thin coatings. However, the application of pulsed bipolar DC allows for controlled interruption of the process and thus the arc duration; the pulse form can also be changed. Both of these features allow the heat conditions during treatment to be controlled, and thus the coating

composition and structure changed. It has been also reported that the pulsed bipolar AC source provides obtaining denser and more uniform oxide ceramic layers with a fine-grained microstructure than that of layers produced using AC source (Yerokhin, Shatrov, Samsonov, Shashkov, Leyland, & Matthews, 2004).

The electrolyte constituents can be adjusted according to the substrate metal being anodized. Colloidal solutions of sodium or potassium silicate, as well as multicomponent electrolytes based on silicates, are widely used in MAO processes. Besides silicates, the solution can contain substances, e.g. NaF, NaOH or KOH that increase the electrolyte conductivity and/or provide the oxide layer with stabilising elements, e.g. borates, glycerine or carbonates and modifying components, e.g. aluminate, tungstate or vanadate (Yerokhin, & et al., 1999). Silicates enhance the deposition rate, but can result in porosity and lower coating hardness. Phosphates and other additions contribute to coating hardness and to surface smoothness.

For specific purposes fine powders of hard, high melting point materials and/or dry lubricants (for improved friction and wear), and/or colouring agents (for optical properties and decoration) can be introduced into the electrolytes, to integrate cataphoretic effects with the oxidation process.

It is also common for the bath to be enclosed and for air to be pumped through the bath. This helps to agitate the electrolyte, as well as ensuring that there is sufficient dissolved oxygen in the system. A mechanical mixer may also be used. The enclosure is typically an earthed steel frame with an insulating base plate and electrical interlocks on the access doors to ensure the safety of operators.

3.4 Coating Formation

3.4.1 Electrochemical Characteristics

Yerokhin, & et al. (1999) overviewed electrical plasma process and described the current-voltage characteristics during the MAO process. Figure 3.2 represents the

current-voltage characteristics of a system where oxide film formation occurs during the MAO process. Firstly, the passive film previously formed begins to dissolve at point U_4, which, in practice, corresponds to the corrosion potential of the material. Then, in the region of repassivation U_4-U_5 a porous oxide film grows, across which most of the voltage drop now occurs. At point U_5, the electric field strength in the oxide film reaches a critical value beyond which the film is broken through due to impact or tunnelling ionisation. At point U_6, the mechanism of impact ionisation is supported by the onset of thermal ionisation processes and slower, larger arc-discharges arise. In the region U_6-U_7, thermal ionisation is partially blocked by negative charge build-up in the bulk of the thickening oxide film, resulting in discharge-decay shorting of the substrate. Above the point U_7, the arc micro-discharges occurring throughout the film penetrate through to the substrate and (since negative charge blocking effects can no longer occur) transform into powerful arcs, which may cause destructive effects such as thermal cracking of the film.

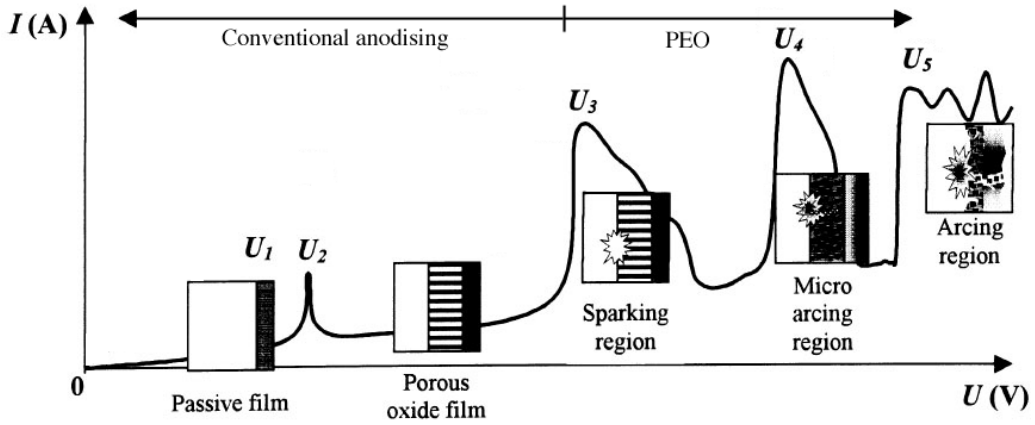


Figure 3.2 The current-voltage diagram for MAO processing regime (Yerokhin, & et al., 1999)

3.4.2 Discharge Characteristics

Each discharge is the result of a localised loss of dielectric stability (Van, & et al., 1977). This occurs at flaws in the barrier film. At these flaws, the breakdown field strength is surpassed, and an electron avalanche occurs through the oxide.

Limited studies suggest that the material within a discharge channel (1-10 μm in diameter) is heated up to about 10^4 K (Klapkiv, 1995). The time period for heating is estimated to be as little as 1 μs (Yerokhin, & et al., 1999), and local pressures of up to 1000 MPa (10.000 atm) (Yerokhin, Nie, Leyland, & Matthews, 2000) can be inferred. Under these conditions, the material is locally ionised and plasma-chemical reactions occur. The strong electric field draws anionic components into the channel from the electrolyte, while magnesium and other alloying elements are drawn into the channel from the substrate to be oxidised.

Yerokhin, Snizhko, Gurevina, Leyland, Pilkington, & Matthews, (2003) studied microdischarge using real time imaging of the micro arc oxidation process. By digital video imaging study of AC MAO of an aluminium alloy, both the spatial characteristics of individual micro-discharges and their collective behaviour throughout the oxidation process are analysed. The typical evolution of micro discharge is shown in Figure 3.3 from which four consecutive stages of the MAO process can be distinguished. During stage I, intense gas evolution is clearly observed, along with some luminescence at the surface (Figıre 3.3(a)), which is eventually replaced by the onset of a bluish glow discharge around the sample. In stage II, the discharge tends to contract at the areas of the surface with maximum electric field intensity and appears, therefore, in the form of moving discrete white microdischarges (Figure 3.3(b)), though a uniform glow background remains visible for sometimes. After about 10-12 min of treatment, the process gradually enters stage III, where the appearance of the microdischarges becomes more pronounced (Figure 3.3(c)). Further MAO processing makes some of the microdischarges yellow, larger and slower moving, which becomes a major feature of the process in stage IV (Figure 3.3(d)).

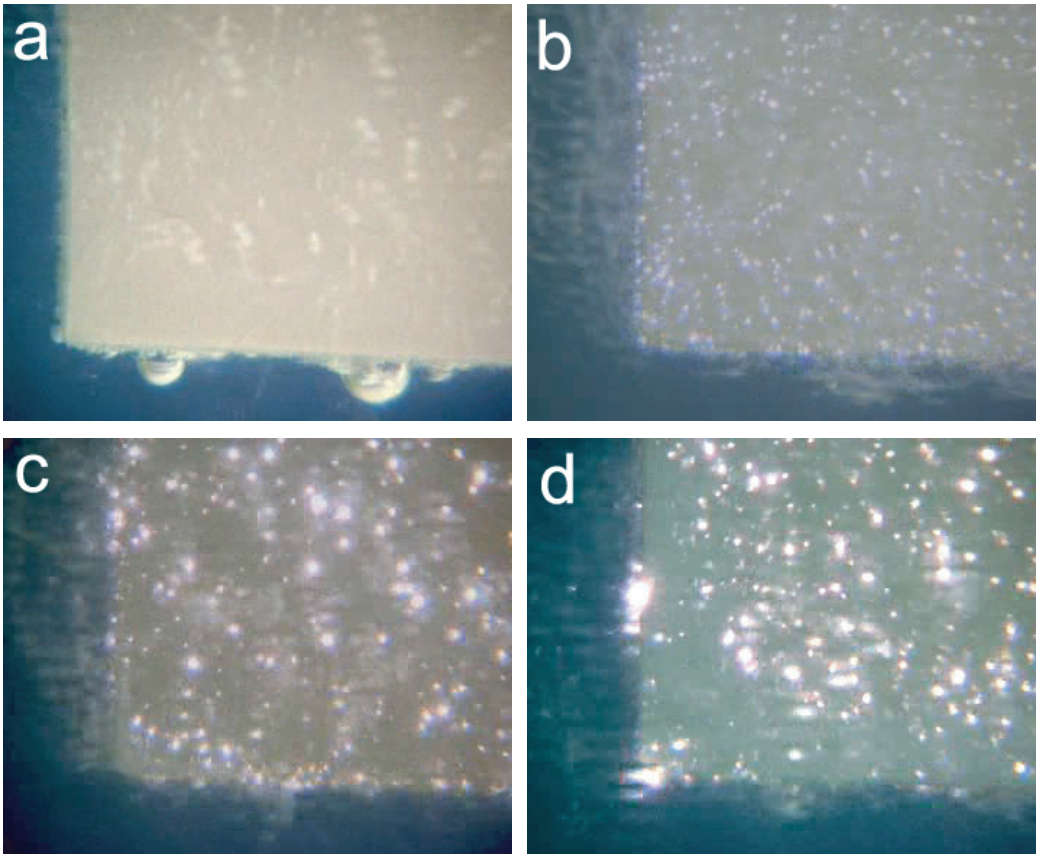


Figure 3.3 Sample surface appearance at various stages of the coating formation process: (a) 0.5 min; (b) 10 min; (c) 35 min, and (d) 65 min (Yerokhin, Snizhko, Gurevina, & et al., 2003).

3.4.3 Electrochemistry of MAO

With ionic current of the layer growth passing through oxide layer, there are two parallel processes for MAO coating growth: the electrochemical and the plasma chemical mechanisms (Yerokhin, Lyubimov, & Ashitkov, 1998).

The electrochemical formation of surface oxide layers can occur through different mechanisms. Unfortunately, there are few studies of the electrochemical formation of surface oxide layers in the electrolyte used for MAO such as aqueous solutions of inorganic polymers-silicates, aluminates, phosphates, etc. It has been proposed in early studies that these layers are formed by the polycondensation of adsorbed anionic complexes of an electrolyte due to dehydration under the action of an electric field (Ikonopisov, Girginov, & Machkova, 1979). Therefore, the processes associated with ionic diffusion can be ignored, so the coating composition can be formed only

from the anionic complexes of an electrolyte when considering the electrochemical formation of oxides in such electrolytes.

In recent decade, several works report on systematic investigation into the effects of process parameters on the growth kinetics and thermodynamics and associated changes in the structure, phase composition and mechanical properties of surface layers by the MAO treatment (Sundararajan, & Krishna, 2003), (Yerokhin, Lyubimov, & Ashitkov, 1998) and (Snizhko, Yerokhin, Pilkington, Gurevina, Misnyankin, Leyland, & Matthews, 2004). However, existing data in the literature on the energy efficiency of MAO are quite controversial.

For revealing the basic electrochemical processes, a series of experiments on micro arc oxidation has been performed by Yerokhin & et. al. In their early experiments (Yerokhin, Leyland, & Matthews, 2002). they attempted to develop a MAO process for deposition of aluminium titanate coatings on titanium. However, the process parameters chosen for that work (application of AC MAO mode and a complex aluminate-base electrolyte) allowed only qualitative consideration of current distribution (Figure 3.4). According to the Figure 3.4, oxide layer formation is induced both by the ionic component of the current which is transmitted via surface discharges and by the anodizing current passing across the surface which is free of discharges. Other components of the current cause secondary electrochemical processes which lead to liberation of electrode gases (e.g. H_2 and O_2), accumulation of H_2O_2 in the electrolyte, anodic dissolution of the titanium metal and electrothermally induced metallurgical processes in the surface layer. The anodising current is supported by electrolyte anions which (in alkaline aluminate solutions) are predominantly OH^- and AIO^{2-}. Since the aluminate ions in particular are relatively unstable, they can in alkaline media partly interact with water and/or create complex anions between themselves, forming either mono- or poly-hydroxyanions, e.g. $AI(OH)_4^-$ or $Al_n(OH)_{4n+2}^{(n+2)-}$. On the surface of the titanium electrode, the above anions can take part in the following anodic processes (Yerokhin, Leyland, & Matthews, 2002):

$$Ti^{4+}+2OH^{-}+2H_2O=TiO_2+2H_3O^{+} \quad (3.1)$$

$$Ti^{4+}+4AlO_2=TiO_2+2Al_2O_3 \quad (3.2)$$

$$Ti^{4+}+4Al(OH)_4^{-}=TiO_2+Al_2O_3+2Al(OH)_3+5H_2O \quad (3.3)$$

In their subsequent work, a quantitative evaluation of the rates of the major anodic processes is performed in a different approach, in which a simplified model situation should first be considered for the rate evaluation of partial processes during MAO (Snizhko, & et al., 2004). The experimental facility developed for this purpose comprises the following functions: (i) recording and analysis of the main electrical characteristics of the process, (ii) determination of the oxide layer thickness, (iii) anodic gas collection and composition analysis and (iv) electrolyte analysis to determine anodically dissolved metal. The experiments were performed on aluminium anodes oxidized in a model dilute alkaline solution (0.5 to 2 g/l KOH) under conditions of galvanostatic DC MAO, for which basic electrochemical processes were considered, such as oxide film growth, anodic dissolution and oxygen liberation. Four different stages of the MAO process were identified, characterized by various rate proportions of the partial anodic processes, i.e. (i) anodizing, (ii) anodizing with anodic dissolution, (iii) anodizing, dissolution and oxygen liberation and (iv) plasma electrolysis (Figure 3.5).

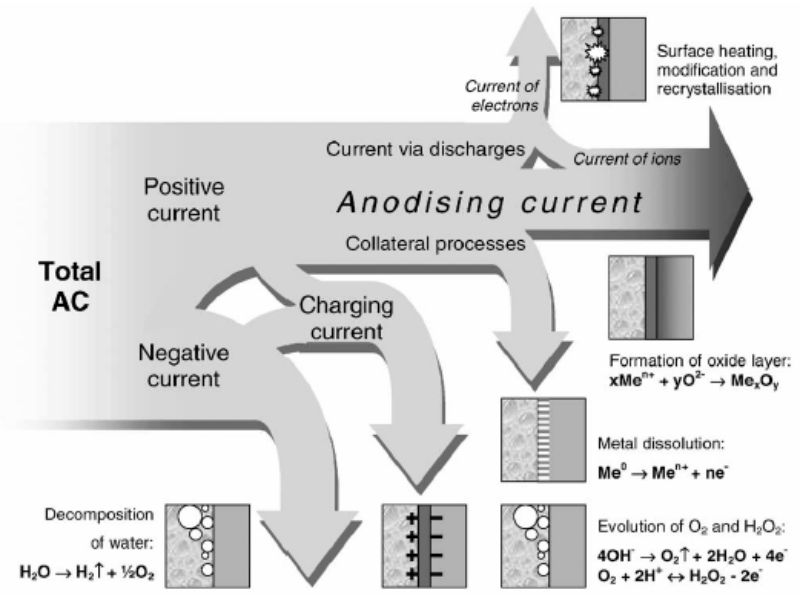


Figure 3.4 Schematic diagram of current distribution during the PEO treatment of metals in AC mode (Yerokhin, Leyland, & Matthews, 2002).

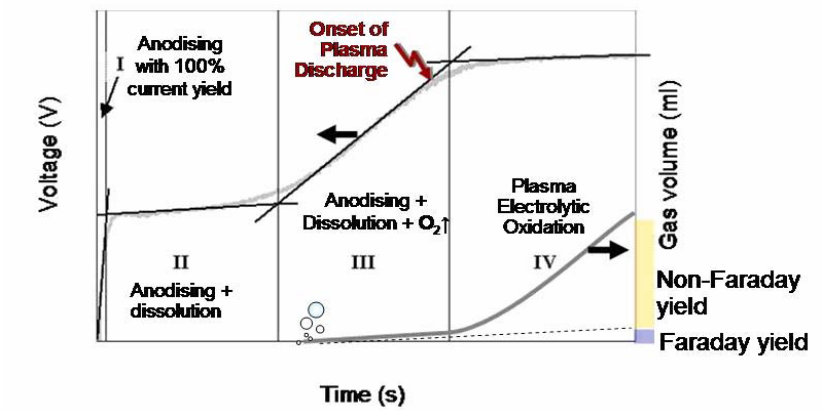


Figure 3.5 Typical evolution of voltage and gas volume with time for galvanostatic DC MAO of Al in dilute KOH solutions (Snizhko, & et al., 2004).

The overall current efficiency of the oxide film formation was estimated to be in the 10 to 30% range (depending on the process conditions). It was also found that the film growth rate decreased significantly with increasing electrolyte concentration, since the rate of anodic dissolution increased. Oxygen evolution was shown to be the main electrochemical process at the potentials corresponding to the plasma stages of the electrolysis (oxygen current yields 60 to 80%). Estimations of the process efficiency were carried out, assuming that the partial processes of oxide film growth, dissolution and gas evolution on the surface are governed by the Faraday's law. The overall rate of oxygen liberation at the anode exceeds the Faraday yield, which is probably due to the radiolytic effect of the plasma discharge on the adjacent electrolyte volume. The processes associated with this effect were considered and reaction routes leading to non-Faradic formation of gaseous products quantified, including (a) generation of free electrons with corresponding H_2O^+ vacancy formation, (b) quadratic recombination of the vacancies with the electrolyte anions and water molecules resulted in formation of free OH radicals followed by (c) their annihilation due to either acceptor trapping or recombination processes, resulting in the formation of excessive gaseous products (Snizhko, & et al., 2004).

Duan, Yan, & Wang, (2007) were studied the growth process of MAO films formed on AZ91D Mg alloy in silicate solution. They prepared coatings at various processing durations and characterized the coatings using scanning electron

microscopy (SEM) with energy dispersive analysis of X-rays (EDAX) to propose a growth mechanism. The electrochemical reactions occurring at magnesium electrode/electrolyte interface are presented in this study. However, they investigated the effect of microstructural changes in substrate alloy on the formation of MAO coating.

When growing a MAO coating on magnesium, the bulk of the coating consists of magnesium oxide (MgO; periclase), although oxides of all the other alloying elements are likely to become incorporated into the coating as well. Hsiao, & Tsai, (2005) explained the electrochemical reactions that occurred on AZ91 Mg alloy during the MAO process are as follows;

$$Mg - 2e^- = Mg^{2+} \quad (3.4)$$

$$Al - 3e^- = Al^{3+} \quad (3.5)$$

$$Mg^{2+} + 2OH^- = Mg(OH)_2 \quad (3.6)$$

$$Al^{3+} + 3OH^- = Al(OH)_3 \quad (3.7)$$

$$Al^{3+} + 2AlO^{2-} = MgAl_2O_4 \quad (3.8)$$

$$Mg(OH)_2 = MgO + H_2O \quad (3.9)$$

3.4.4 Plasma discharge models and plasma chemistry

Apart from the electrochemical, the plasma chemical processes were discussed (Sundararajan, 2003), (Yerokhin, Lyubimov, & Ashitkov, 1998), (Snizhko, Yerokhin, & et al., 2004) and (Ikonopisov, et al., 1979). The plasma chemistry of the surface discharges is quite complex in nature, involving, on one hand, reactions between electrons, molecules of water and electrolyte anions and on the other, atoms and ions of the metal electrode. An important consequence of the occurrence of surface discharges is the development of metallurgical processes in the growing oxide layer, which are induced by the heat liberated in discharge channels from electron avalanches. Cycles of instantaneous local heating and cooling of the areas of the oxide layer in close proximity to a discharge channel lead to the melting, quenching and recrystallisation of the substances deposited onto the surface. As a

result, decomposition of magnesium hydroxide to MgO, formation of complex compounds based on the Mg-O system, can occur. The direction and intensity of these processes depend on the density and power of the discharges which are known to be defined by thickness of the oxide layer, so that the thicker the layer the less frequent yet more powerful and extended the discharges become.

In the plasma reaction, the key is the formation of microdischarge. Several microdischarge formation models have been proposed. For the first model (Yerokhin, Lyubimov, & Ashitkov, 1998), (Klein, 1978) and (Albella, Montero, & Martinez-Duart, 1987), the microdischarges appear as a result of oxide film dielectric breakdown in a strong electrical field (Figure 3.6(a)). The breakdown is treated as a 'streamer propagation' due to the electron avalanche effects induced by film dopants and structural defects. Three main steps can be discerned in the breakdown process. In the first step, the discharge channel is formed in the oxide layer as a result of the loss of its dielectric stability in a region of elevated conductivity. This region is heated by generated electron avalanches up to temperatures of ~10^4 K. Due to the strong electric field (of the order of ~10^6 V/m), the anionic components of the electrolyte are drawn into the channel. Concurrently, owing to the high temperature, aluminium and alloying elements are melted out of the substrate and enter the channel. Thus, a plasma column (plasmoid) is formed as a result of these processes. In the second step, plasma chemical reactions take place in the channel. These lead to an increase in pressure inside the channel. So the plasmoid expands to balance it. At the same time, separation of oppositely charged ions occurs in the channel due to the presence of the electrical field. The cations are ejected from the channel into the electrolyte by electrostatic forces. In the last step, the discharge channel is cooled and the reaction products are deposited onto its walls.

The second group of models (Yerokhin, Snizhko, Gurevina, & et al., 2003) considers each microdischarge as a gas discharge occurring in a micropore of the oxide film (Figure 3.6(b)). The formation of a gas phase in the pore (and discharge ignition in it) is believed to be induced by an initial dielectric breakdown of a barrier layer in the bottom of the micropore.

An alternative model of microdischarge formation was proposed (Figure 3.6(c)) based on analogy with the contact glow discharge electrolysis originally studied by Hickling, & Ingram, (1964). In their work, a glow discharge was observed at the interface of the electrolyte and a thin vapour sheath was formed at the surface of a platinum wire anode at $U^{+} \geq 420V$. In the case of an aluminium anode, however, the role of the vapour sheath is played by the gas bubbles accompanying the oxidation process and the discharge; therefore, it seems as if it is disintegrated into a number of microdischarges. Nevertheless, it is important to recognize that the common condition of discharge initiation in both cases appears to be electron emission from the electrolyte surface (partial cathode) into a gaseous phase, rather than dielectric breakdown of the growing oxide film. It should also be noted that free electrons might appear initially at the oxide-electrolyte interface in strong electrical fields, regardless of the presence of any gas/vapour phase, due to the ionization of anions and molecules of water. The free electrons would then immediately participate in a series of reactions with water, resulting in the formation of gaseous products (H_2 and O_2), thus providing the necessary conditions for maintenance of a stable plasma discharge environment.

Another model worthy of consideration for AC MAO discharge is the dielectric barrier discharge, which has recently been reviewed by Wagner, Brandenburg, Sonnenfeld, & et al., 2003). Similar to MAO, the barrier discharge operates under AC polarization and atmospheric pressure conditions, with one electrode covered by a thin dielectric film. The barrier discharge usually operates in a filamentary mode, for which the phenomenology is similar in appearance to a microdischarge in MAO, except that the barrier discharge occurs during both positive and negative half-cycles. Furthermore, unlike the discharge in MAO, dielectric barrier discharges cannot be produced using simple DC polarization.

A.L. Yerokhin et. al found that the above models do not fit the spatial, temporal and electrical characteristics of microdischarge phenomena which were observed in their investigations (Yerokhin, Snizhko, Gurevina, & et al., 2003) and (Yerokhin, Snizhko, Gurevina, Leyland, Pilkington, & Matthews, 2004). A new model is

suggested based on the analogy with contact glow discharge electrolysis. The model assumes the possibility of free electron generation and glow discharge ignition in the gaseous media at the oxide-electrolyte interface, which leads to heating, melting and quenching of the underlying oxide layer.

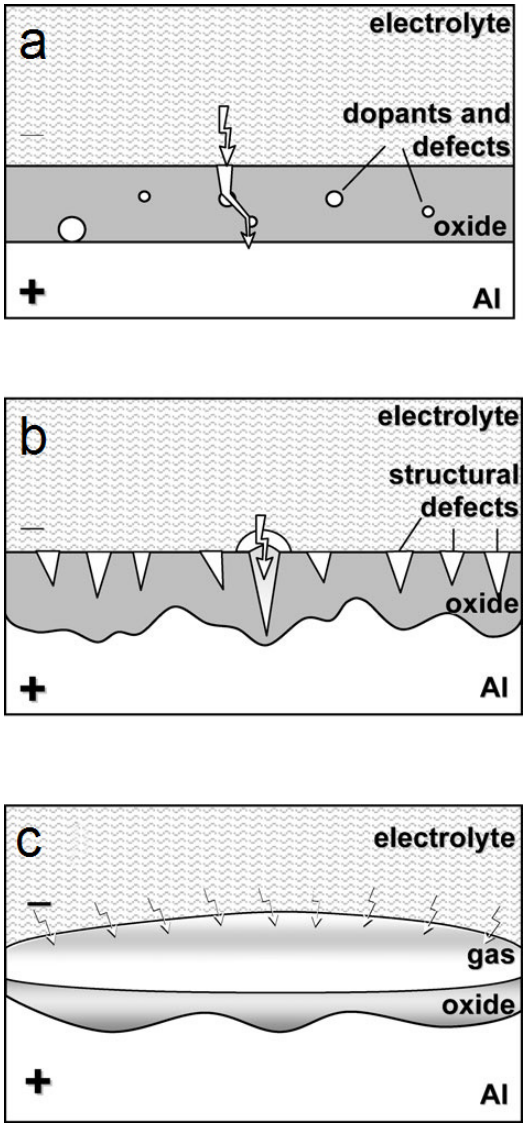


Figure 3.6 Schematic illustration of models describing the appearance of surface discharge during anodic oxidation of AI: (a) model of the oxide film dielectric breakdown, (b) discharge-in-pore model and (c) model of contact glow discharge electrolysis adapted for the presence of an oxide film on the metal surface (Yerokhin, Snizhko, Gurevina, Leyland, Pilkington, & Matthews, 2003).

3.5 Tribological Properties of MAO Coatings

Various studies (Dearnley, & et al., 1999), (Dahm, & et al., 2009), (Merstallinger, & et al., 2003), (Mistry, & et al., 2008), (Krishna, & et al., 2006) and (Rao, & et al., 1997) have demonstrated a superior performance of MAO coatings on aluminium for tribological applications and there has been a subsequent surge in the use of MAO for aluminium applications, only a few published reports are available on the tribological studies of MAO treated magnesium alloys and thus lacks the information for enabling the use of magnesium on tribo-applications.

In recent years, there are several studies concerning the wear behaviour of MAO coatings on Mg alloys were published. Guo, Wang, Liang, Xue, & Yan, (2009) investigated the tribological properties of the MAO coating on AM60B magnesium alloy under engine oil lubrication at temperature up to 120 C and the relationship between temperature and tribological performance of the MAO coating and magnesium alloy was analyzed in detail. They reported that MAO coating exhibited significantly higher wear resistance and relatively lower friction coefficient when compared with uncoated Mg alloy under oil-lubricated conditions at normal oil temperature (80–120 °C). Excellent tribological performance of the MAO coating can be attributed to the higher hardness and micro-porous structure. They indicated that the micro-pores and micro-dimples surface structure of the MAO coating could demonstrate a positive and beneficial effect to the oil-lubricated wear performance. The contact angle of lubricated oil on the MAO coating surface was less than 30°, in such case, the oil drop had great tendency to enter into pores or holes by capillary action. These pores and dimples on MAO coating can act as natural reservoirs for oil lubricants and enable oil easier to penetrate into the contact area, thus promote the lubricant spreading and enhance the complete formation of boundary lubrication film from the contact. This can effectively prevented direct contact between the steel ball and the MAO coating, and resulted in a low and stable friction coefficient and higher wear resistance of MAO coating.

Srinivasan, Blawert, & Dietzel, (2009) studied the effect of coating thickness and normal load on the wear behaviour of MAO-coated AZ91 magnesium alloy. They performed dry sliding wear tests on MAO coatings of 10 and 20 μm thickness. They used ball on disc oscillating tribometer with an AISI 52100 steel ball of 6 mm diameter as static friction partner. The wear tests were performed at ambient conditions (25±2 ^{o}C) at three different load levels, viz., 2N, 5N and 10N with an oscillating amplitude of 10 mm and at a sliding velocity of 5 mm/s for a sliding distance of 12m. Test results showed that MAO coatings improved the wear resistance of AZ91 magnesium alloy significantly. For MAO coatings of 10 μm thickness, the increasing normal load damaged the coating and complete removal of coating was observed. This was attributed to the deformation of substrate at higher initial stress levels which causes the cracking and flaking-off of the coating especially when it is thin. When the coating thickness increased, the load bearing capacity of coating improved so that the wear resistance increased.

In another study published by Liang, Guo, Tian, Liu, Zhou, & Xu, (2005), the effect of KF addition into the electrolyte on the tribological behavior of MAO coating on magnesium alloy was investigated. Test results showed that KF contributes to decrease the pore diameter and surface roughness and increase the compactness of the MAO coating. At the same time, it leads to changes in the phase compositions of the coatings as well. Consequently, the coating formed in the electrolyte with KF has a higher surface hardness and better wear-resistance than that formed in the electrolyte without KF.

MAO coatings exhibit great adhesion to the substrate, because it is a conversion process rather than a deposition method. But these coatings usually have a porous top layer which increase material loss during sliding motion of machine parts. In this case, this layer is removed away from the surface to decrease surface roughness or different surface layers can be applied to improve frictional properties. There are numerous studies on the formation of composite surface structures combined with a base MAO coating. Liang, Wang, Hu, & Hao, (2007) obtained duplex MAO/DLC coating on AM60B magnesium alloy using combined micro-arc oxidation and

filtered cathode arc deposition. The MAO coating served as an intermediate layer for the DLC top coating, providing necessary hardness and load support for the soft magnesium alloy substrate. The deposition of DLC film onto MAO coating improves the dry friction behaviour significantly. The friction coefficient of MAO/DLC composite structure shows three times less value than polished MAO coating. Hutchins et al. investigated the corrosion and mechanical performance of MAO coatings on AZ91D magnesium alloy with different post-treatments such as sol-gel, silicate, e-coat and powder-coat. They applied scratch test to evaluate the adhesion properties. The two sealants, sol-gel and silicate, increased the scratch resistance of MAO coating approximately 30% and e-coat by nearly 3 times. For powder coat, the scratch test indenter did not detach the MAO, even with maximum loading, providing the best adhesion strength.

3.6 Commercialisation of MAO Process

Mg and its alloys can be anodized by either DC or AC current in nearly any solution which can carry current and not dissolve the magnesium or the coating faster than it can form. However just a few of them have reached industrial importance. These are listed in the following text.

3.6.1 Magoxid-Coat Process

The Magoxid-Coat process has his origins in Russia and was further developed by AHC-Oberflächentechnik GmbH in Germany. The plasma is generated by an external power source in a slightly alkaline electrolyte near the surface of the work-piece (anode). The discharging (by arcing) and formation of oxygen plasma in the electrolyte causes partial short-term surface melting and ultimately the formation of an oxide-ceramic layer. In order to obtain coatings that have little or no inherent colour, that can be easily coloured, and that provide a satisfactory adhesive base for lacquering or subsequent processing, a low-alkali aqueous electrolyte is used. It contains borate or sulphate anions, phosphate and fluoride or chloride ions. The pH value is adjusted between 5 to 11, but preferably 8-9 is employed. Especially

appropriate for buffering the electrolytes are amines that react weakly in alkaline solutions and generally have dissociation constants of 10^{-2}–10^{-7}. These amines, in particular cyclic amines such as pyridine, β-picoline, piperidine and piperazine, are generally dissolving readily in water. Other satisfactory water-soluble amines that can be employed are for example sodium sulphanilate, dimethylamine, ethylamine, diethylamine and hexamethylenetetramine. Methenamine is especially preferred. For anodizing, a direct current is applied and is either briefly turned off or its polarity is completely reversed to allow the formation of manganese phosphate and magnesium fluoride and optionally magnesium aluminate on the surface. It is preferable to work with a voltage that increases to 400 V. The current density is in particular 1-2 A/dm^2. The present process is patented in the United States (U.S. Patent 4,978,432A), Europe (EP 0333048B1) and Japan (JP5-51679B4). Further information about the process can also be found in these patents (Blawert, Dietzel, Ghali, & Song, 2006).

3.6.2 Tagnite Process

The Tagnite Coating System was developed in the 1990's in the USA by Technology Applications Group Inc. as a chromate-free anodic surface treatment, and they claim that it is providing significantly more corrosion and abrasion resistance than any chromate based coating. Like typical anodizing coatings, the part to be coated is connected to a conductive rack which carries the part throughout the coating process. Once placed in the Tagnite coating tank, the rack and part become the anode and the tank holding the electrolyte serves as the cathode (Blawert, Dietzel, Ghali, & Song, 2006).

The electrolyte used to form the coating is an alkaline solution clear in colour, containing no chromium (VI) or other heavy metals and operates below room temperature (40° to 60 °F). It mainly consists of an aqueous solution containing hydroxide, fluoride and silicate species which are also incorporated into the layer. The rectifier used to apply Tagnite was specifically designed for the coating. It employs a unique waveform optimized for the coating process. To ensure maximum

corrosion resistance and high dielectric strength, the Tagnite coating is applied at voltages exceeding 300 V DC (Blawert, Dietzel, Ghali, & Song, 2006).

3.6.3 Keronite Process

Keronite technology was conceived in Russia and developed in the UK by Isle Coat Ltd, a subsidiary of CFB plc. The process results in hard, wear-resistant coatings, which also provide good corrosion resistance and a good thermal barrier. Light alloys such as aluminium, titanium and magnesium can all be treated, and the technology offers significant improvements compared with traditional methods such as hard anodizing or coating with nickel-silicon carbide. Keronite also compares favourably with spark-anodizing processes currently being developed around the world (Blawert, Dietzel, Ghali, & Song, 2006).

Keronite is also using a plasma electrolytic oxidation process that transforms the magnesium metal surface into ceramic oxides by a plasma discharge in an electrolytic bath. The plasma discharge converts magnesium into complex ceramics by oxidation of the surface, elementary co-deposition and fusion of the ceramic layer. Thereby the plasma discharge is localized in a thin surface layer and magnesium is not subjected to thermal exposure. Electrical bipolar (positive and negative) pulsed electrical current of a specific wave form in a proprietary electrolyte is used, and the electrical current creates the plasma discharge near the surface of the part to be coated. Energy consumption of 0.01-0.03 KWh/micron dm^2 of the process depends on the controllable coating rate which ranges from 1 to 5 microns/min at a temperature between 20 and 50 °C. The electrolyte is a non-hazardous, low concentrated alkaline solution (98% demineralized water, chrome and ammonia free), which can easily be disposed (Blawert, Dietzel, Ghali, & Song, 2006).

CHAPTER FOUR
EXPERIMENTAL STUDIES

4.1 Purpose

It is known that the structural and mechanical properties of MAO coatings such as porosity, surface roughness and hardness influence the tribological behaviour. In this study two different MAO coatings of 10 μm and 25 μm thickness on AZ91D and AM60B magnesium alloys were obtained using Keronite G2 power supply unit in an alkaline electrolyte with low concentrations of KOH, K_3PO_4 and $NaAlO_2$. Thus it is allowed to study both the effect of coating thickness and substrate type on the tribological behaviour and mechanical properties of MAO coatings which were produced in the same electrolyte.

Scanning Electron Microscope (SEM) equipped with Energy Dispersive X-ray Spectrometer (EDS) was used to determine the surface morphology and elemental composition of MAO coatings. The crystallographic phase analysis and identification of MAO coatings were carried out by X-ray diffraction (XRD). High resolution surface profilometer was used for mapping of the 3-Dimensional surface features and measuring surface roughness. Adhesion strength of coatings was evaluated using scratch test. Tribological behaviour of MAO coatings under dry sliding against 100Cr6 steel ball was investigated using ball-on-plate test configuration.

4.2 Materials

In order to prepare MAO coatings, AZ91D and AM60B magnesium alloys in the form of plates provided by TUBITAK Marmara Research Center Materials Institute TURKEY, were used as substrates. Nominal compositions of the alloys used in this study are given in Table 4.1.

Table 4.1 Nominal composition of key alloying elements in magnesium alloys

Material	Composition (wt. %)			
	Mg	Al	Zn	Mn
AZ91D	Bal.	9	0.74	0.17
AM60B	Bal.	5.9	0.05	0.27

4.3 MAO Process

4.3.1 Substrate Preparation

The magnesium alloy plates (20 mm x 20 mm x 3 mm) were ground to 2400 grits using SiC sandpapers and pre-treated using proprietary chemicals at various stages in order to degrease, clean and activate the surface of magnesium alloy. The pre-cleaning procedure included three stages of cleaning in various acids and alkali bath followed by rinse in DI water baths after each subsequent cleaning. The pre-treatment procedure is shown in Figure 4.1.

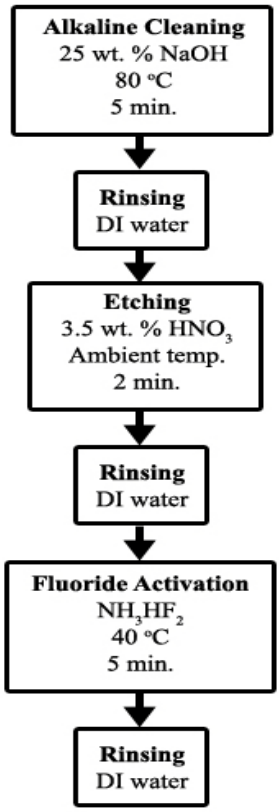


Figure 4.1 The pre-treatment procedure of magnesium alloys

The etching step serves to remove surface layers such as oxides covering the surface thus the potential distribution on the surface becomes equalized. Fluoride activation forms a passive MgF_2 layer which inhibits extreme anodic dissolution of the substrate magnesium alloy during the initial anodising process.

4.3.2 Electrolyte Preparation

As mentioned before, there are several electrolyte constituents involved for coating valve metals (aluminium, magnesium, titanium and zirconium etc.). Colloidal solutions of sodium or potassium silicate, as well as multicomponent electrolytes based on silicates, are widely used in MAO processes. Besides silicates, the solution can contain substances that increase the electrolyte conductivity (e.g. NaF, NaOH or KOH) and/or provide the oxide layer with stabilising elements (e.g. $Na_2B_4O_7.10H_2O$, glycerine, Na_2CO_3 or K_2CO_3) and modifying components (e.g. $NaAlO_2$, $Na_6P_6O_{18}$).

In the present work, the electrolyte conductivity was increased using KOH chemical. Modifying components, K_3PO_4 and $NaAlO_2$, were also used to form spinel phases such as $Mg_2Al_2O_4$ besides MgO which is less stable in corrosive medium than spinel phases. The electrolyte used in MAO process was prepared by dissolving the chemicals in DI water. The chemical ingredients and properties of electrolyte used in MAO process are listed in Table 4.2. The pH and conductivity of electrolyte were measured using Mettler Toledo pH/conductivity dual meter.

Table 4.2 The chemical ingredients and properties of electrolyte used in MAO process

Electrolyte constituents		**pH at ambient.**	**Conductivity**
Chemical	**Amount (g/l)**	**temp.**	**(mS/cm)**
KOH	2		
K_3PO_4	10	12.5	25.3
$NaAlO_2$	5		

4.3.3 Preparation of MAO Coatings

The equipment used for MAO process is similar to that used for conventional anodising, but more complex, primarily due to the need for higher potentials and controlled pulses of current. In essence, however, it consists of an array of capacitor banks, which can be charged by a 50 Hz three phase supply. Their capacitance may be controlled to produce pulses of positive and negative charge to a pair of electrodes at frequency of 50 Hz. More complex equipment can provide control of the pulse frequency.

The schematic of MAO process is given in Figure 3.1. Keronite G2 MAO system with a 25kW pulsed bipolar DC power supply, heat exchanger and circulating pump was used for coating magnesium alloys. In the MAO process, magnesium alloy specimen was primarily used as the anode while the stainless steel was primarily used as the cathode. Magnesium alloy plates attached with an insulated aluminium bar were dipped into the alkaline electrolyte and fixed to copper bus bar.

In MAO process, the electrolyte is circulated through a heat exchanger, cooled by chilled water-glycol mixture, filtered and returned into the tank together with air, via a whistle pump, which also serves to ultrasonically agitate the electrolyte. Agitation helps to provide sufficient dissolved oxygen in the electrolyte. The electrolyte temperature was kept below 30ºC during operating. If it is allowed to heat up beyond 30ºC, the coating process can be faster but the electrolyte is depleted of active ingredients much more rapidly.

The MAO process parameters are shown in Table 4.3. In the present work, two different process durations, 7 and 15 minutes, were chosen to obtain coatings with 10 μm and 25 μm thickness respectively.

Table 4.3 MAO process parameters

Substrate	Electrical parameters			Treatment time (min.)		Electrolyte parameters		
	Power supply	Initial current density (A/dm^2)				Temperature (^oC)	pH	Conductivity (mS/cm)
		K10	K25	K10	K25			
AZ91D AM60B	Pulsed bipolar DC	20		7	15	12-25	12.6	25.3

K10: 10 μm MAO coating, K25: 25 μm MAO coating

The MAO equipment was used in auto-control mode, whereby the effective capacitance of the pulsed power supply is set to a fixed value. This maintains a constant current output through MAO process. In the initial stage of MAO process the current density was adjusted to 20 A/dm^2 to achieve the breakdown voltage more rapidly, thus it is allowed to obtain coatings of the same type in a shorter time. At breakdown voltage (~200 V) the discharges begin to appear on substrate surface. As time progresses, the voltage slowly rises due to the increasing coating thickness.

4.4 Coating Thickness Measurement

The coating thickness measurements were carried out by using Mitutoyo Digiderm 1100 coating thickness gauge. Also, the thickness values were verified by performing cross-sectional analysis of coatings in SEM.

4.5 Microstructural Investigation

4.5.1 SEM Observation

The structural and semi-quantitative elemental analyses of MAO coatings were investigated using JEOL 6060 SEM with energy dispersive X-ray analysis (EDX) attachment. The SEM is equipped with a LaB6 gun and is capable of operating as a conventional high vacuum SEM. The SEM is fully equipped with a range of secondary electron (SE) and back-scattered electron (BSE) detectors. EDX analyses

including light elements are done semi-quantitatively. Corrections for atomic number, absorption and fluorescence (ZAF) are achieved through a virtual standard calibration routine.

Because the coatings have low electrical conductivity, a thin conductive film of gold-palladium was produced on MAO coatings by Polaron Range SC7620 sputter coater (at 9 mA for three minutes) and low accelerating voltages were used during SEM analysis.

4.5.2 X-ray Diffraction

The phase compositions of MAO coatings were determined using Rigaku X-ray diffractometer with CuKα radiation as excitation source. The signal was recorded at 0.02^{o} steps. Peak fitting was then applied to the diffraction traces and, from the angular positions of peaks, the crystalline phases present could be identified by comparison with reference patterns from the Powder Diffraction File (PDF) from the International Centre for Diffraction Data.

4.5.3 Surface profilometry and roughness measurement

The surface roughness and 3D mapping of MAO coatings were obtained by Ambios XP-2 high resolution surface profilometer. However, the wear profiles of specimens were obtained to calculate the material loss due to sliding wear.

This method uses an instrument that amplifies and records the vertical motions of a stylus displaced at a constant speed by the surface to be measured. The XP-2 surface profilometer has the lowest mass and inertia stylus assembly to minimize tip/sample interaction with stylus loads as low as 0.05 mg. The stylus is mechanically coupled to a proprietary optical deflection height-measurement sensor. Thus it is provided to measure nano-scaled surface features such as ridges or grooves. The stylus arm is loaded against the sample and either the stylus is scanned across the stationary sample surface using a traverse unit at a constant speed or the sample is

transported across an optical flat reference. As the stylus or sample moves, the stylus rides over the sample surface detecting surface deviations by the transducer. It produces a signal corresponding to the vertical stylus movement. This signal is then amplified, conditioned, and digitized.

The surface data (vertical vs. horizontal displacement) was recorded by a computer. Afterwards, the 3D surface map and roughness value of coatings were obtained using TrueMap and TrueSurf software respectively.

4.6 Hardness measurement

The hardness of MAO coatings and bare magnesium alloys were measured by Shimadzu HMV-1 microhardness tester. This equipment uses a diamond Vickers tip which can be loaded from 0.025 N to 20 N for various durations. For measuring the hardness of MAO coatings, the diamond tip was loaded onto the surface at 0.1 N for 10 s. After the tip was unloaded, the diagonals of Vickers mark was measured using optical microscope already placed on the tester. The minimum unit of diagonal length measurement is 0.01 μm (when the objective lens is x40), thus high-accuracy measurement is possible. In order to calculate the adhesion strength of coatings, brinell hardness values of magnesium alloys were also measured using ball indenter with 2 mm diameter at 20 kg normal load.

4.7 Scratch Test

The adhesion strength of MAO coatings was measured by Shimadzu scanning scratch tester SST-W101 equipped with a standard off-line Zeiss metallographic microscope. In this technique, load on a Rockwell C diamond tip with radius of stylus (R) of 15 μm was linearly increased from 0 mN to 98 mN at loading speed of 1 μm/s and scratch speed of 2 μm/s as the diamond is drawn across the surface of coating. The testing temperature and humidity were recorded at 20 ^{o}C and 60 % respectively. After scratch testing of coatings, the scratch was examined with an optical microscope and the cartridge output-test force graphs were analyzed.

As the applied test force is increased gradually, the coating at certain point chips off. This causes an acoustic emission signal which is recorded as cartridge output. Detecting acoustic emission signals allows to determine a critical force (Wc) at which the coating detached from substrate. The cartridge output represents the percentage of the indentation of stylus into the coating as a function of increasing test load. Normally, the critical force can be used as the adhesion of the coating. However, in the case that a hardness of the substrate has been known, the following equation can also show adhesion strength (Shimadzu Co., 2003);

$$F = H / [(\pi R^2 H - W_c) / W_c]^{1/2} \qquad (4.1)$$

where F is adhesion strength (N/mm^2), H is Brinell hardness of substrate (N/mm^2), R is radius of stylus (mm) and W_c is the critical force (N).

4.8 Wear Test

Dry sliding wear tests of uncoated and MAO coated magnesium alloys were performed using Plint TE-88 multi-station friction and wear test machine under ball-on-plate test configuration at a frequency of 2 Hz. The selected stroke length, applied normal force and the consumed total wear distance were 10 mm, 12 N and 100 m respectively. The 100Cr6 steel bearing ball (HV830) with 10 mm diameter was used as counter-body. All wear tests were repeated three times to minimize the deviation in test results. The wear scars of bearing balls were investigated using optical microscope and the equations (4.2) and (4.3) were used to determine the volume loss of steel ball (ASTM G133, 2005).

$$Vp=(\pi h/6).[(3D^2/4)+h^2] \qquad (4.2)$$

where h is the height of material removed (mm) and D is the effective diameter of ball wear scar (mm).

$$h=R-[R^2-(D^2⁄4)]^{1/2} \quad (4.3)$$

where R is the original ball radius (mm).

For uncoated magnesium alloys, the wear scar on the steel ball was not flat enough to be measured by the optical microscope. Hence the volume loss was given as the material volume loss of uncoated magnesium alloys. The cross-sectional area of the wear scars of uncoated magnesium alloys was calculated using Ambios XP-2 surface profilometer and multiplied by the stroke length in order to obtain the material volume loss of uncoated magnesium alloys.

CHAPTER FIVE
RESULTS AND DISCUSSION

5.1 Substrate Characterisation

Aluminium is one of the most important alloying elements that dissolve easily in magnesium. Several systems contain aluminium up to 10 wt.%, e.g., AZ, AE, AM and AS. Figure 5.1 shows the Mg-Al system. Above the solubility limit $Mg_{17}Al_{12}$ (β phase), a brittle intermetallic, precipitates out. The solubility limit of aluminium at the eutectic temperature is 11.5 at.% (12 wt.%) and falls to about 1% at room temperature. Consequently, the $Mg_{17}Al_{12}$ plays a dominant role in determining the properties. The commercial alloys based on Mg-Al involve further alloying additions of zinc, e.g., AZ91, AZ81, AZ31 and AZ63.

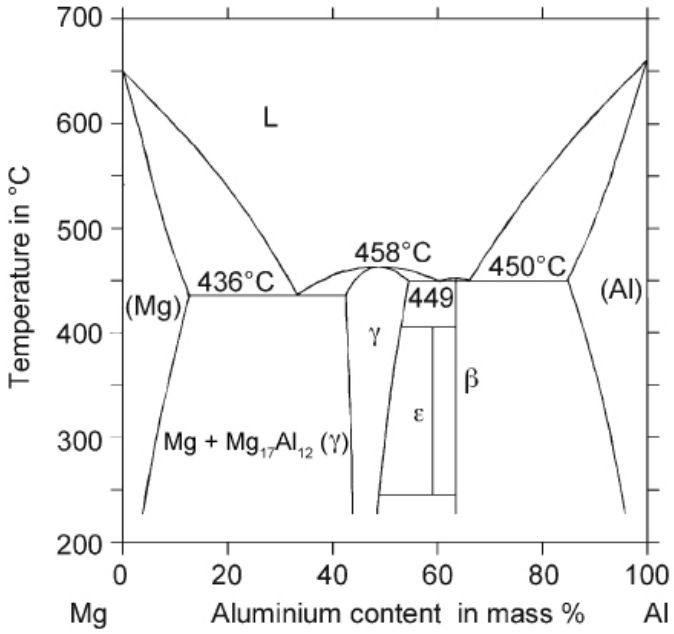


Figure 5.1 Phase diagram of Mg-Al binary alloy

The microstructures of AZ91D and AM60B magnesium alloys used in this study are shown in Figure 5.2. It is found that the microstructures of magnesium alloys consist of two phases. The α-phase (matrix) is a Mg-Al solid solution with the same

crystal structure as pure magnesium. The β-intermetallics ($Mg_{17}Al_{12}$) which have grown from the primary dendrites, are homogeneously dispersed along boundaries of α grains in the fine veined particles. With the increasing Al content in the solid-solution, the β phase increases (Lunder et al., 1989). Thus, increasing amount of $Mg_{17}Al_{12}$ which has a beneficial effect on the strengthening mechanism of the main matrix improves the mechanical properties, e.g., hardness, of magnesium alloys.

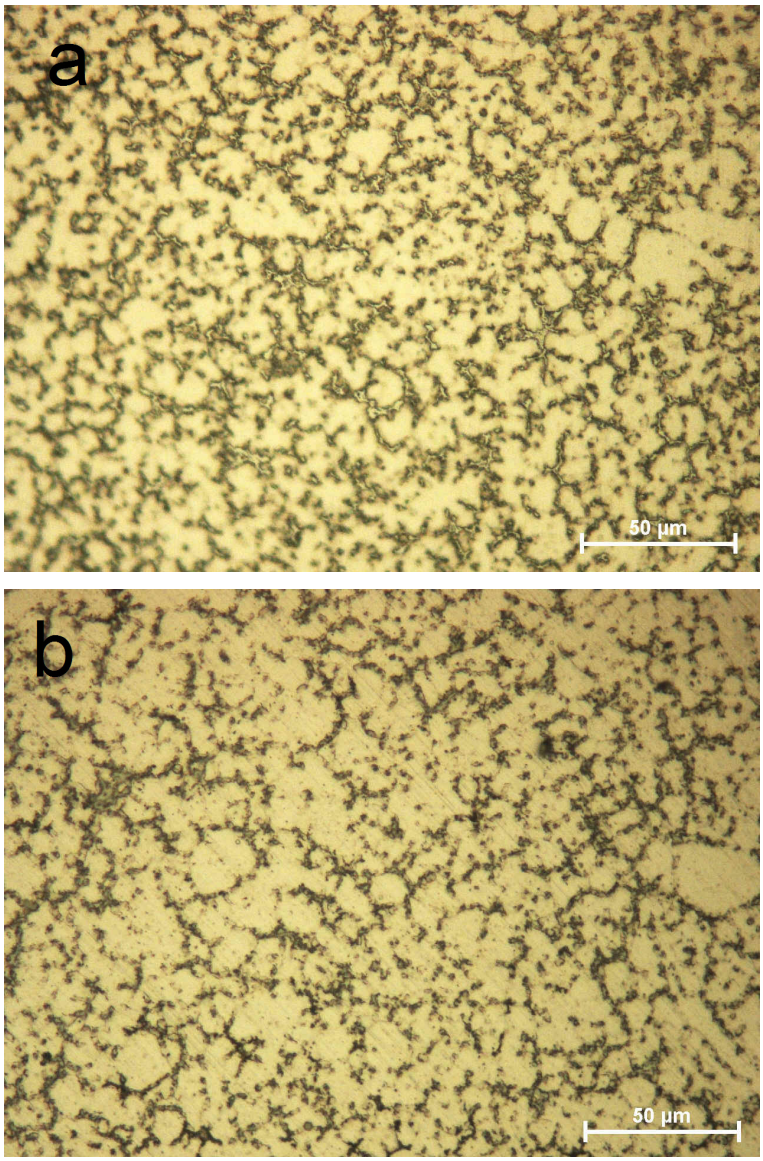
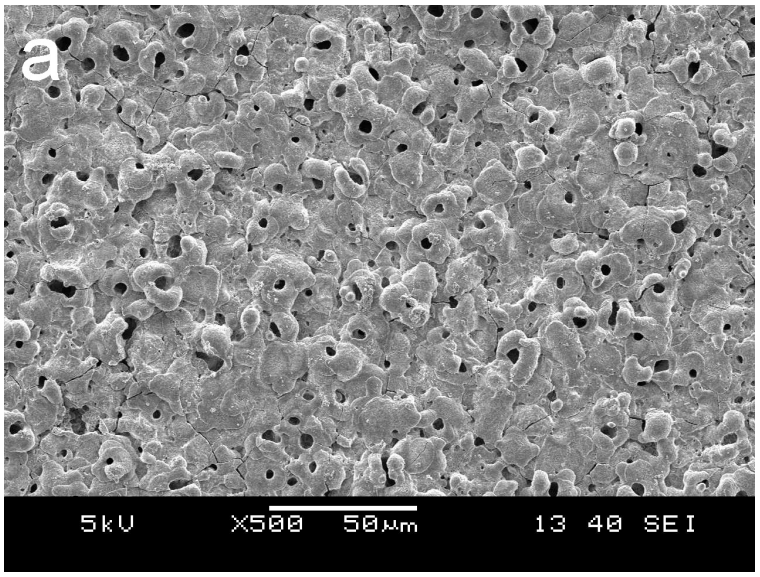


Figure 5.2 The microstructures of (a) AZ91D and (b) AM60B magnesium alloys taken after etching in 90 ml DI water and 10 ml 40% HF solution mixture for 3 seconds. (Dark regions indicate β-intermetallics and light regions indicate α phase)

5.2 Characterisation of MAO Coatings

5.2.1 Surface Morphology and Structure of MAO Coatings

SEM images of a typical surface of the MAO coating taken with secondary electrons (SE) are shown in Figure 5.3. Micro-pores with different sizes are apparent as black contrast holes on the surface. In micro-discharging period these micro-pores acting as a volcano and eruption of molten metal and oxides takes place in these micro-pores. When molten plug exposed to the electrolyte it is quenched and deposited around the micro-pores. It is observed that microarc channels become larger as the coating thickness increases. This is related to the enhanced dielectric strength of thicker coatings. As MAO treatment proceeds, the quantity of microarcs decreases, however, their intensity increases due to the higher energy requirement to break thicker coating. Thus larger micropores were observed on K25 coatings (Figure 5.3b and 5.3d).



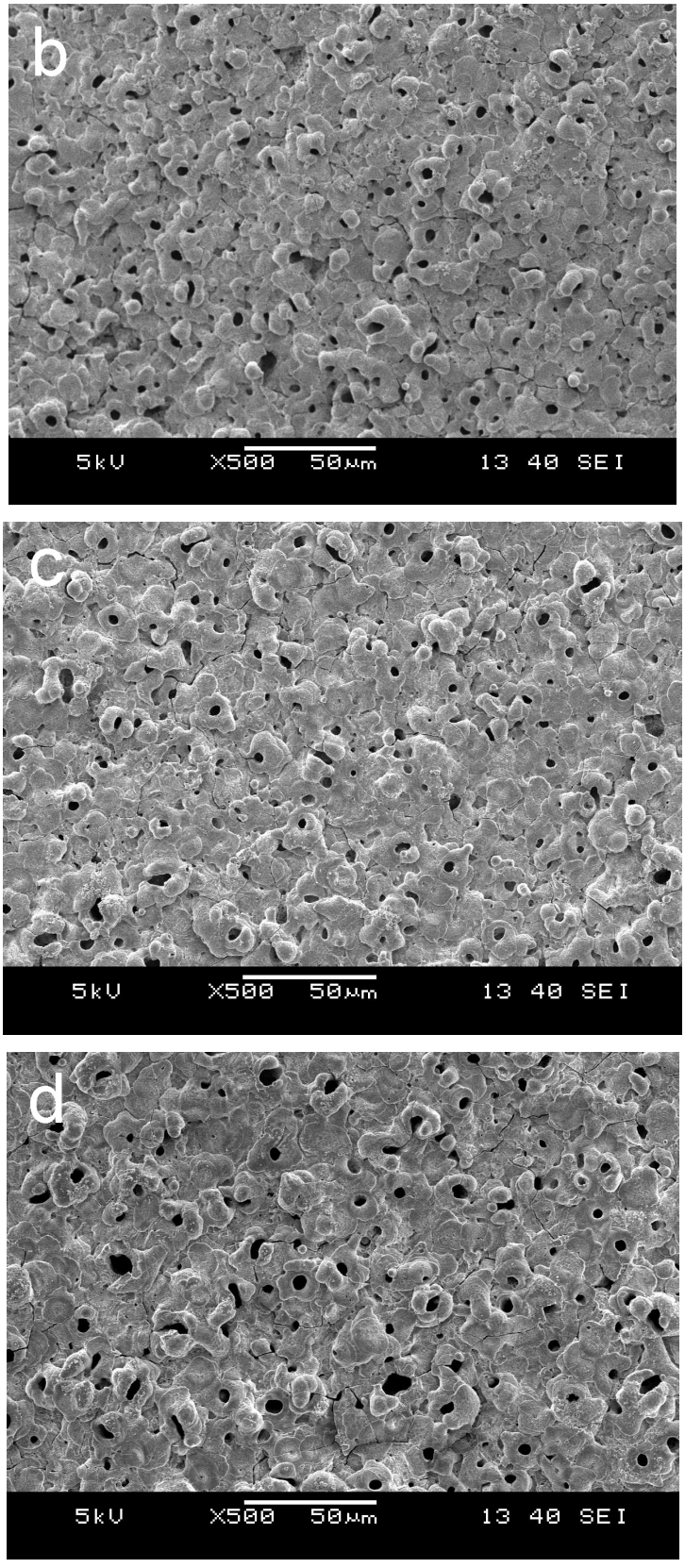


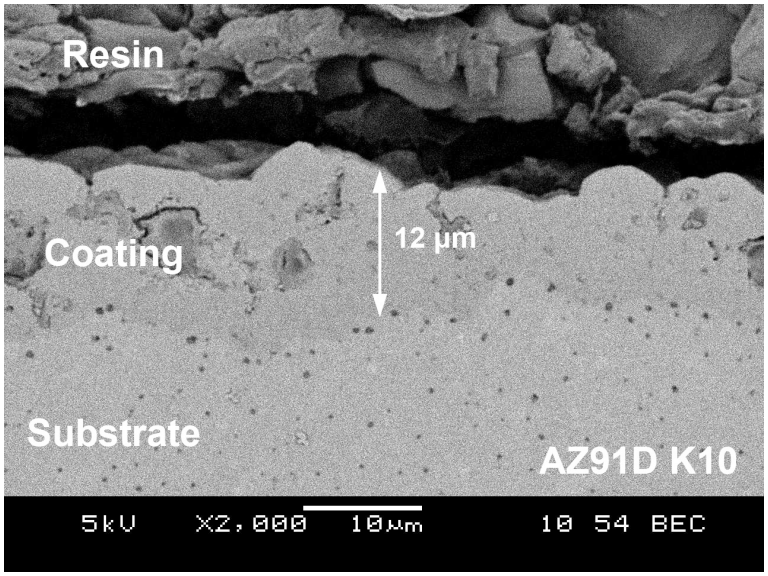
Figure 5.3 SEM images indicating the surface morphology of MAO coatings; (a) K10 and (b) K25 on AZ91D, (c) K10 and (d) K25 on AM60B

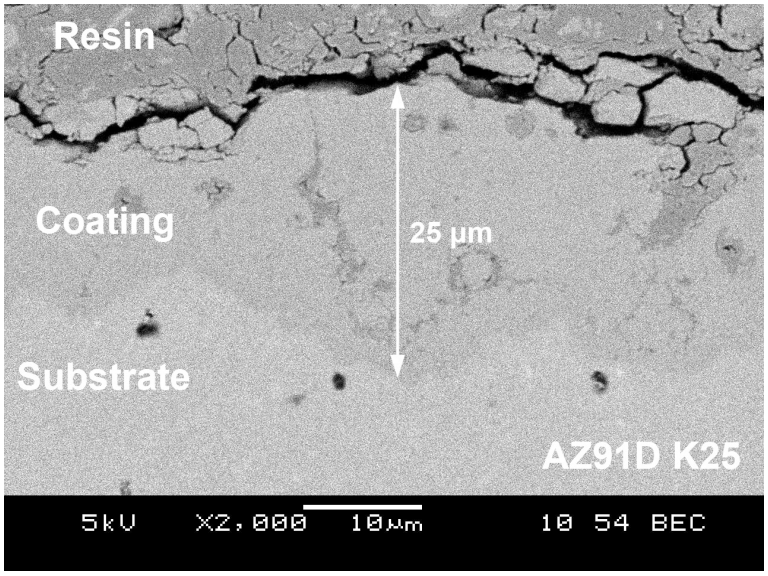
Elemental compositions of the MAO coatings determined by EDS are listed in Table 5.1. Aluminium contents of MAO coatings are greater than magnesium substrates. This can be attributed to the elemental co-deposition from the electrolyte. It is revealed that the anionic components of the electrolyte, e. g. PO_4^{3-}, AlO_2^-, contributed to the coating structure due to the strong electrical field near the electrode surface. Also high percentage of oxygen content in the composition indicates the formation of aluminium oxides besides magnesium oxides. The oxygen content looks similar in all coatings, independent of the formation conditions. However, the measured concentrations of oxygen in the coatings are lower than the real concentrations, as the precision limit of the EDS analysis facility is poor for some light elements.

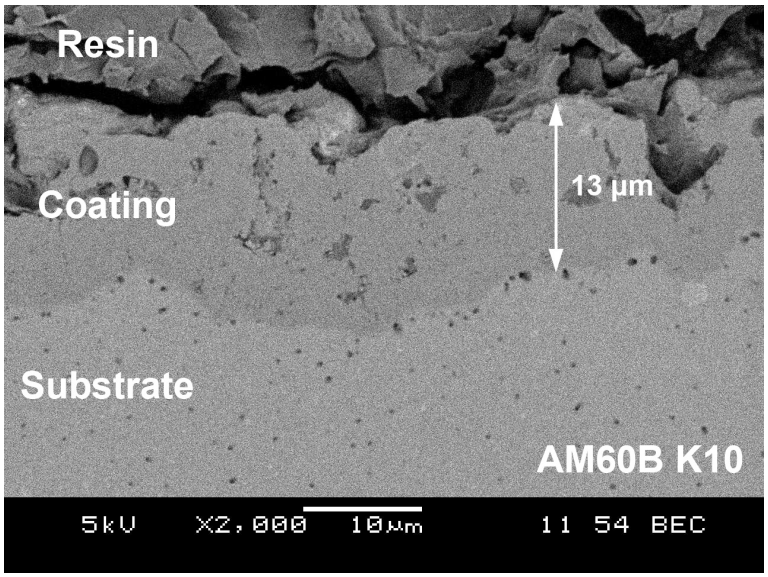
Table 5.1 EDS analysis results of MAO coatings.

Substrate	**Coating Thickness**	**Composition (wt.%)**					
		Mg	**Al**	**O**	**P**	**K**	**Na**
AZ91D	K10	46.8	20.58	25.47	5.33	0.39	1.43
	K25	46.33	21.72	25.21	4.23	0.44	1.35
AM60B	K10	46.81	19.74	24.73	6.75	0.4	1.53
	K25	48.29	20	27.74	2.52	0.22	1.18

The cross-sectional SEM images of MAO coatings are shown in Figure 5.4. The MAO coatings exhibited almost a dense microstructure containing some micropores in the near surface region. The rough surface structure of coatings can provide good adhesion for top-coats like PTFE, sol–gel, PVD and CVD coatings. It is easy to observe a dense barrier layer residing along the coating-substrate interface. This barrier layer is pore-free and provides great adhesion between coating and substrate. It has been also considered that this barrier layer is responsible for the improving corrosion resistance of MAO coatings (Arrabal, Matykina, Hashimoto, Skeldon, & Thompson, 2009).


Resin
Coating
12 µm
Substrate
AZ91D K10
5kV X2,000 10µm 10 54 BEC


Resin
Coating
25 µm
Substrate
AZ91D K25
5kV X2,000 10µm 10 54 BEC


Resin
Coating
13 µm
Substrate
AM60B K10
5kV X2,000 10µm 11 54 BEC

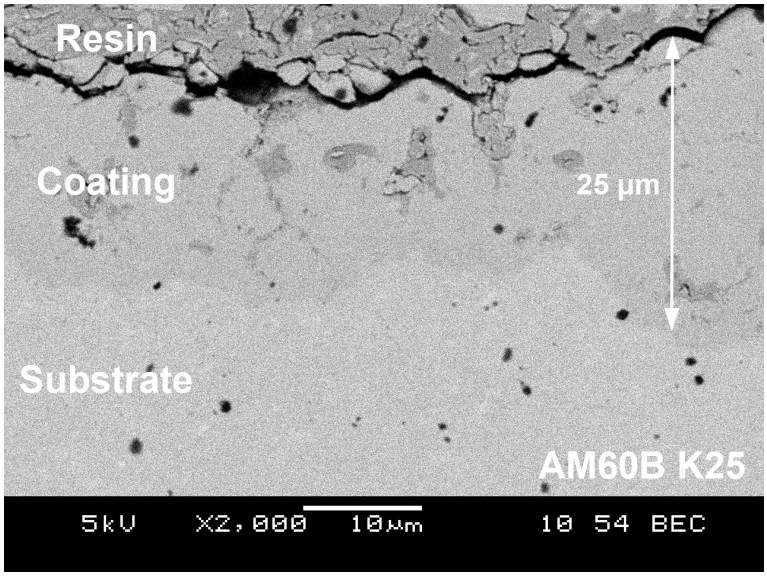


Figure 5.4 The cross-sectional SEM images of MAO coatings

5.2.2 X-ray Diffraction

XRD analysis results of MAO coatings are shown in Figure 5.5. MAO coatings are composed of MgO as main phase and other phases such as $AlPO_4$, $MgAlPO_5$ and $MgAl_2O_4$. Periclase (MgO) was formed via substrate metal oxidation during MAO treatment while $AlPO_4$ and $MgAlPO_5$ phases resulted from the contribution of alkaline electrolyte components into the coating structure. Nevertheless Spinel phase $MgAl_2O_4$ could be formed in the presence of both MgO and Al_2O_3 phases in the coating structure.

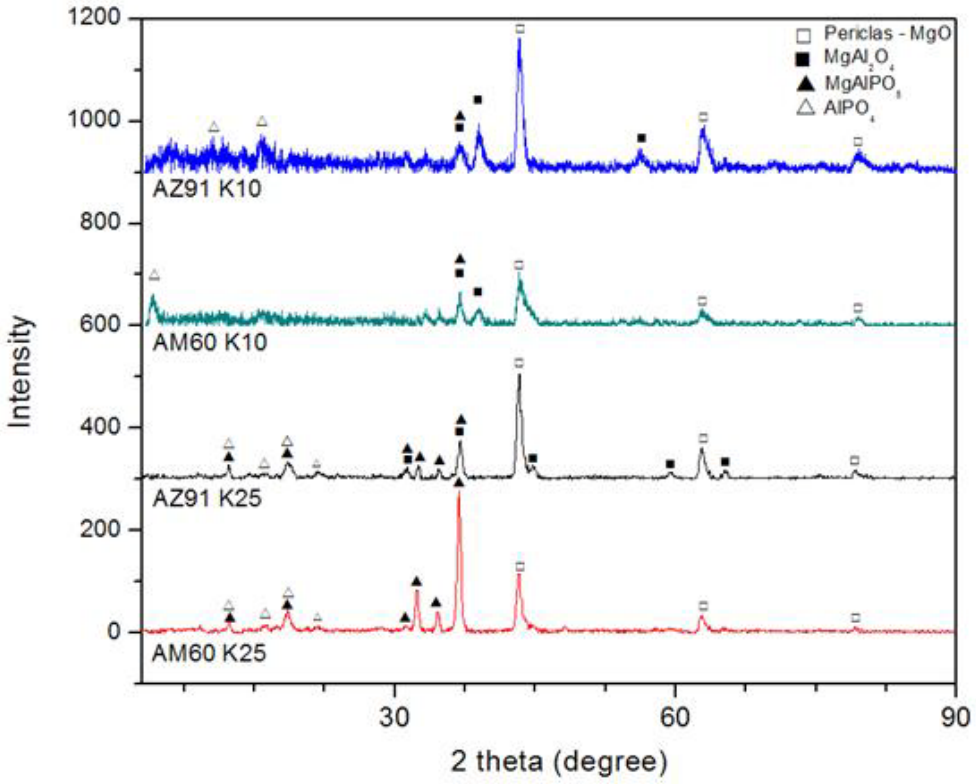
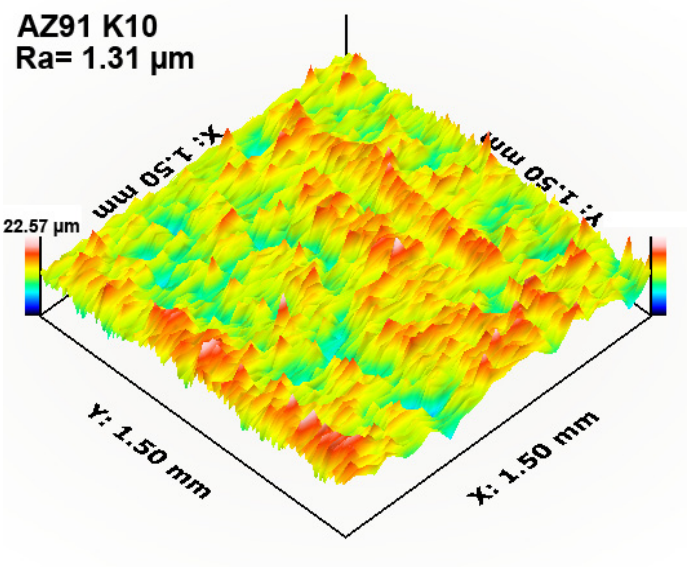
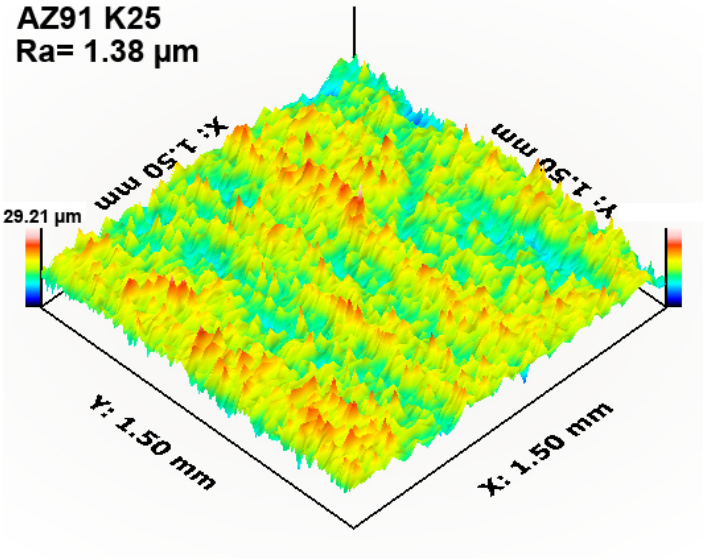


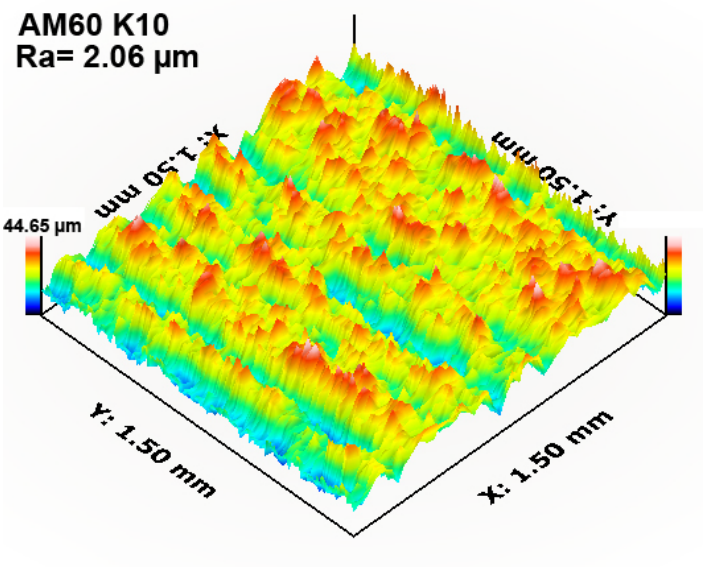
Figure 5.5 XRD results of MAO coatings

5.2.3 Surface profilometry and roughness measurement

Surface 3D profiles of MAO coatings with surface roughness (Ra) values are shown in Figure 5.6. MAO coatings on AZ91D magnesium alloy showed lower roughness values than AM60B alloy. As the coating thickness increased, higher surface roughness values were obtained especially for MAO coatings on AM60B alloy. This is attributed to the larger pore sizes of K25 coatings compared to K10 coatings.


AZ91 K10
Ra= 1.31 µm
22.57 µm
X: 1.50 mm
Y: 1.50 mm
Y: 1.50 mm
X: 1.50 mm


AZ91 K25
Ra= 1.38 µm
29.21 µm
X: 1.50 mm
Y: 1.50 mm
Y: 1.50 mm
X: 1.50 mm


AM60 K10
Ra= 2.06 µm
44.65 µm
X: 1.50 mm
Y: 1.50 mm
Y: 1.50 mm
X: 1.50 mm

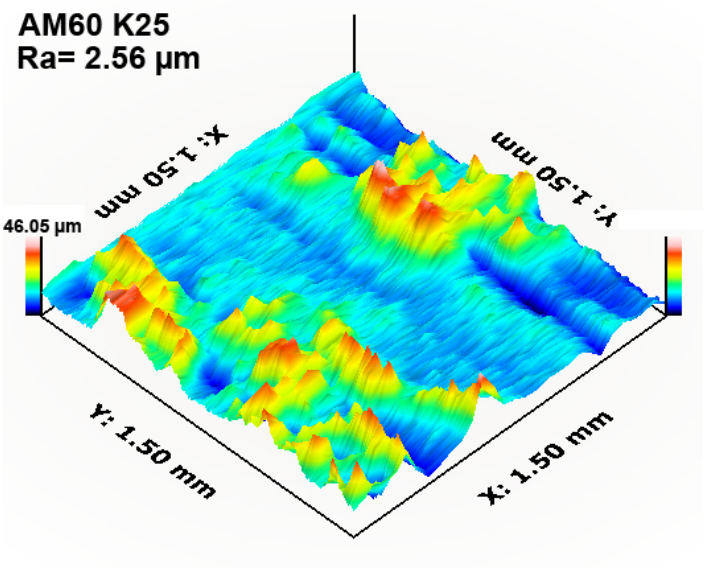


Figure 5.6 Surface 3D profiles of MAO coatings; (a) K10 and (b) K25 on AZ91D, (c) K10 and (d) K25 on AM60B.

5.3 Mechanical Properties

5.3.1 Hardness Measurement and Scratch Test

Microhardness values and scratch testing results of MAO coatings are shown in Table 5.2. Also the cartridge output-normal force graphs which indicate the critical force values for coating removal are given in Figure 5.7. AZ91D magnesium alloy showed higher hardness value than AM60B due to the increasing amount of aluminium in the bulk alloy. Aluminium leads to form intermetallic $Mg_{17}Al_{12}$ phase which precipitates in the grain boundaries and strengthens the main matrix phase owing to its high hardness value. In case of MAO coatings on AZ91D alloy, higher amount of aluminium in the bulk alloy as compared to AM60B may lead to increasing contribution of Al_2O_3 phase into the coating structure via substrate metal oxidation. Thus the MAO coatings on AZ91D showed higher hardness values than AM60B alloy. The hardness values also increased for K25 MAO coatings as compared to K10 coatings. This can be attributed to the increasing load bearing capacity of thicker coatings which may resist to the indenter with less deformation of underlying substrate. Since MAO coating is generated by substrate conversion with plasma chemical oxidation reactions rather than a deposition process, the adhesion of

MAO coatings to substrate metals is mostly considered as being excellent. High local temperatures near the coating/substrate interface during MAO process also lead to significant intermixing and interdiffusional bonding which may also contribute to the adhesion of the coatings (Nie, Leyland, Song, Yerokhin, Dowey, & Matthews,1999). Yerokhin, Nie, Leyland, & Matthews, (2000) showed that the adhesion strength of MAO coatings on Ti6Al4V produced in different electrolyte compositions is affected by hardness, structure and thickness of coatings. The beneficial combination of high hardness and thickness as well as a dense film structure and an extended interface which provided both good load support and adhesion resulted in increasing adhesion strength to the substrate. Even though high hardness may impart brittleness and cause poor adhesion to substrate it is reported that MAO coatings exhibit a fine nano-scaled grain size which may improve the strength and ductility of coating (Nie, Meletis, Jiang, Leyland, Yerokhin, & Matthews, 2002). The MAO coatings formed on AZ91D substrate exhibited greater adhesion strength than AM60B owing to higher hardness values. It is also reported that the increasing coating thickness improves the adhesion of MAO coatings to the substrate alloy (Yerokhin, Nie, Leyland, & et al., 1999). In this study K25 MAO coatings both on AZ91D and AM60B magnesium alloys exhibited higher adhesion strength as compared to K10 MAO coatings. This may be due to structural changes in the interface region, or basically due to greater load bearing capacity and higher hardness of K25 coatings as compared to K10 coatings.

Table 5.2 Mechanical properties of MAO coatings

Substrate	**MAO Coating**						**Uncoated**	
	Critical force Lc2 (mN)		**Adhesion strength (MPa)**		**Microhardness of MAO coating ($HV_{0.1}$)**		**Microhardness of Mg Substrates ($HV_{0.1}$)**	**Brinell Hardness[a]**
	K10	**K25**	**K10**	**K25**	**K10**	**K25**		
AZ91D	35.3	36.4	106	111	406±38	433±49	82	75
AM60B	25.1	26.9	72	78	319±52	368±30	70	62

[a] 20 kg normal load was applied onto the substrates using 2 mm ball indenter.

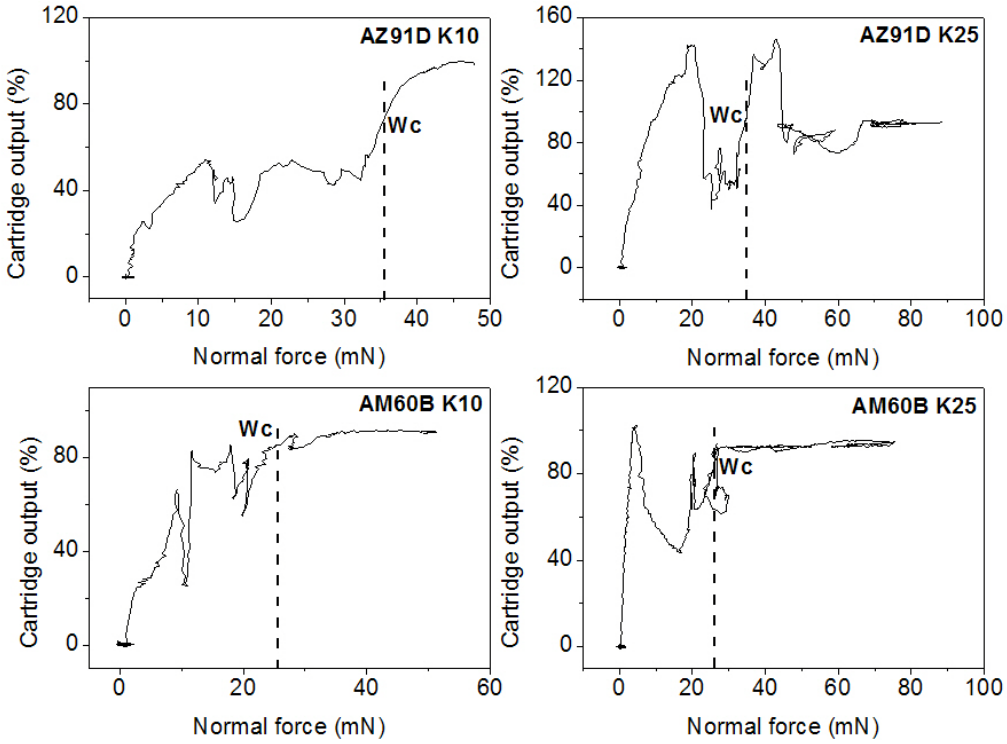


Figure 5.7 Cartridge output-Normal force graphs indicating the critical force values for coating removal

5.4 Tribological Behaviour

5.4.1 Dry Sliding Wear Test

The SEM images of uncoated magnesium alloys tested using ball-on-plate test configuration are shown in Figure 5.8. As the steel ball slid against magnesium alloy substrate, wear particles torn off the surface of substrate and these are adhered onto the steel ball and work-hardened in the latter stages of sliding motion. As a consequence, the increasing hardness of these particles caused ridges and grooves in the wear track. However it is known that magnesium greatly oxidises even in atmospheric conditions and thus oxidative wear mechanism which facilitates abrasive wear could act during sliding motion.

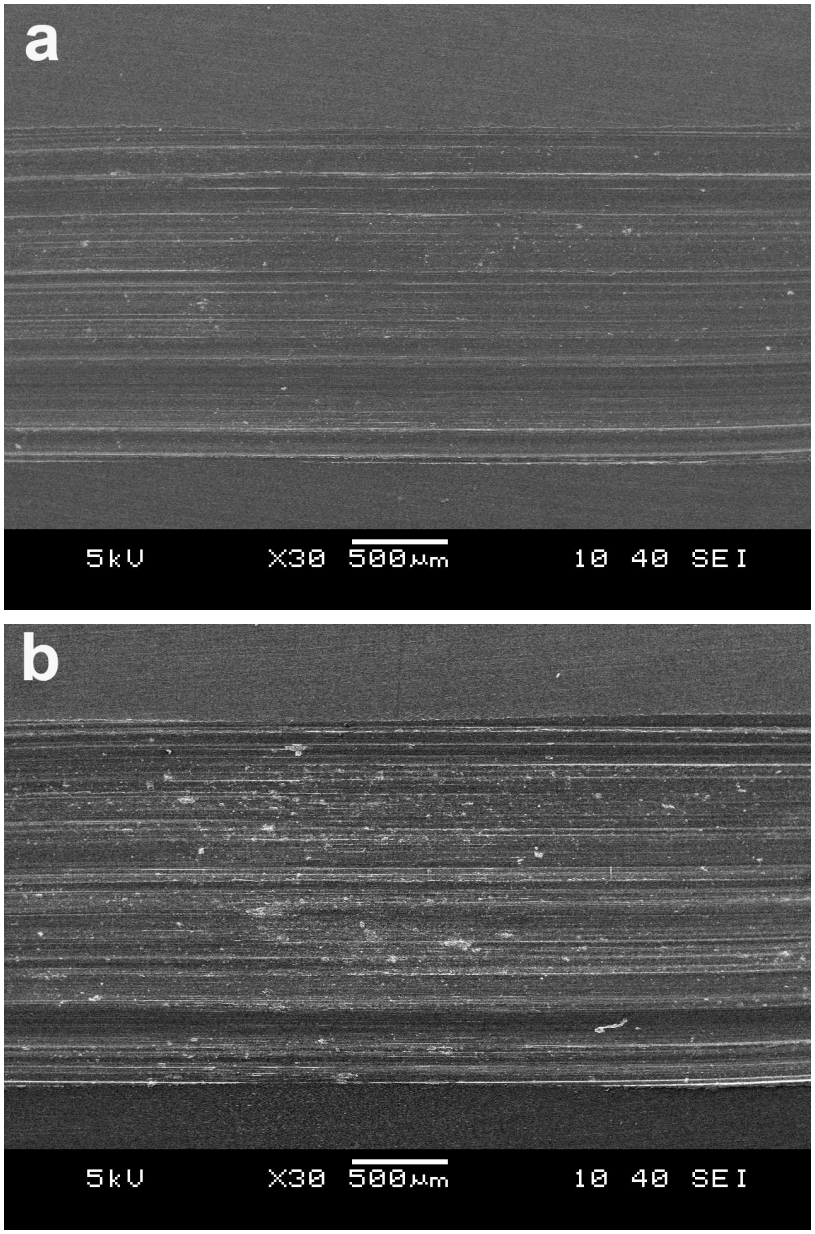
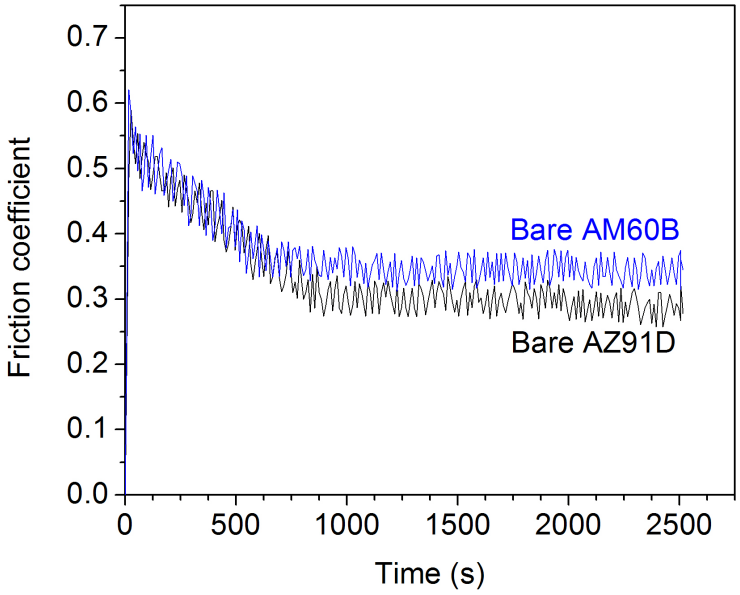
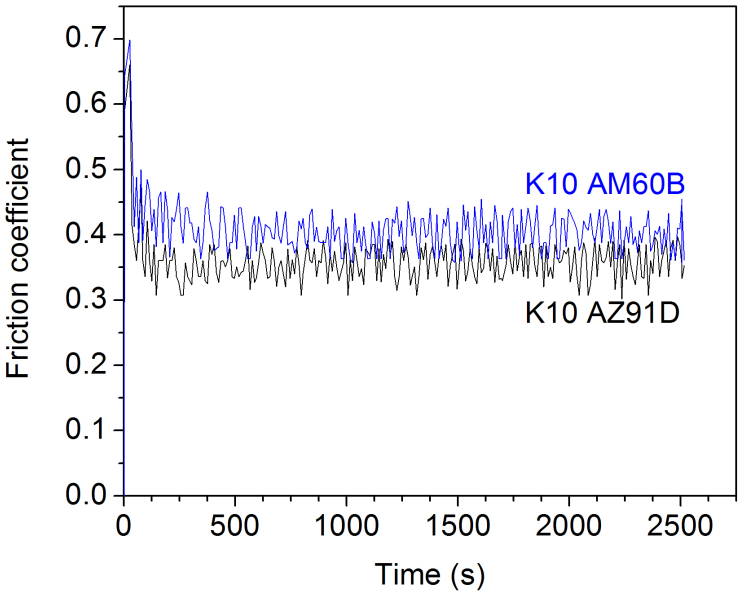


Figure 5.8 The SEM images taken from the worn surfaces of uncoated (a) AZ91D and (b) AM60B alloys

The variation in the friction coefficient is shown in Figure 5.9. For bare magnesium alloys, the friction coefficient increased to ~0.55 in the initial stage of sliding and then decreased almost linearly. Afterwards it remained almost constant around 0.30 and 0.35 for AZ91D and AM60B magnesium alloys respectively. These values are in good agreement with previous studies (Srinivasan, & et al., 2009) and (Blau, & Walukas, 2000). The decreasing friction coefficient is related to the existence of thin oxide film formed on the surface of magnesium alloy. In the initial

stages of sliding, microfracture could take place in the oxide film and the removal of hard oxide film resulted in lower friction coefficient due to establishment of metal-on-metal contact. For MAO coatings, the friction coefficient increased as compared to bare magnesium alloys as a result of different wear mechanisms occurring in the interface region. In all tests AM60B magnesium alloy with and without MAO coating showed slightly higher friction coefficients than AZ91D.





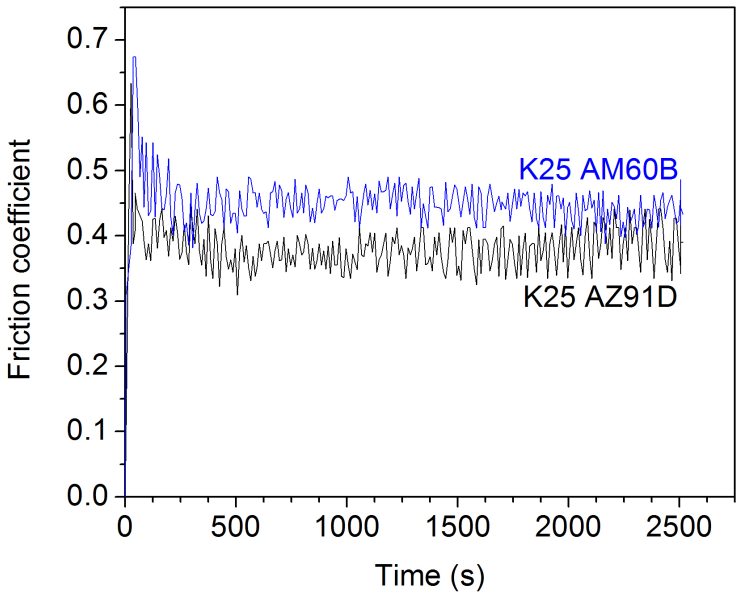


Figure 5.9 Friction coefficients of uncoated and MAO coated magnesium alloys

The wear scar images of the steel balls are shown in Figure 5.10. The scoring marks observed on the steel ball showed that abrasive wear mechanism acted during the sliding motion. Dark regions observed on wear scars can be attributed to the oxidation of steel or particle transfer to the worn surface of steel ball during sliding wear. The abraded surfaces of K10 and K25 MAO coatings on AZ91D alloy are shown in Figure 5.11. In the initial stages of sliding motion the ridges existing on the surface of MAO coatings flattened by the steel ball and the resultant abrasive particles caused excessive wear damage of steel balls. The same type of abrasive wear mechanism was observed both for K10 and K25 MAO coatings. The flattened surface of K25 MAO coating on AZ91D was in smaller size than that of K10 coating indicating the higher wear resistance of thicker coatings. The Fe content in EDS analysis results taken from the flattened region of the coating revealed that particles of steel ball adhered onto the surface of MAO coatings.

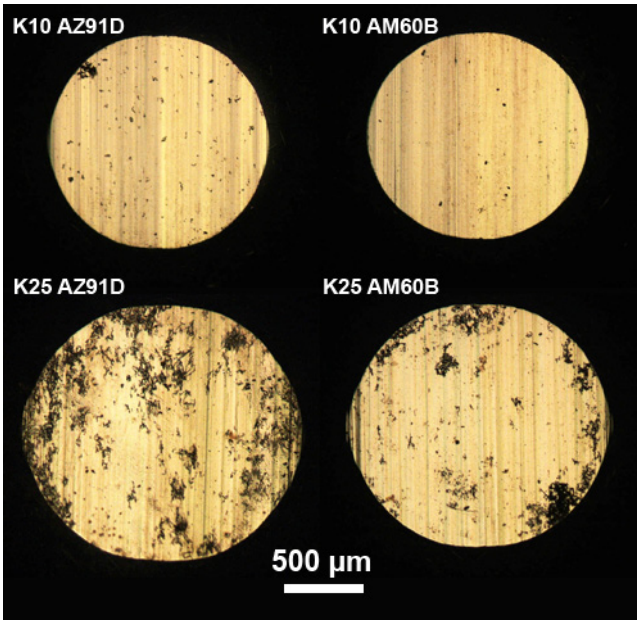
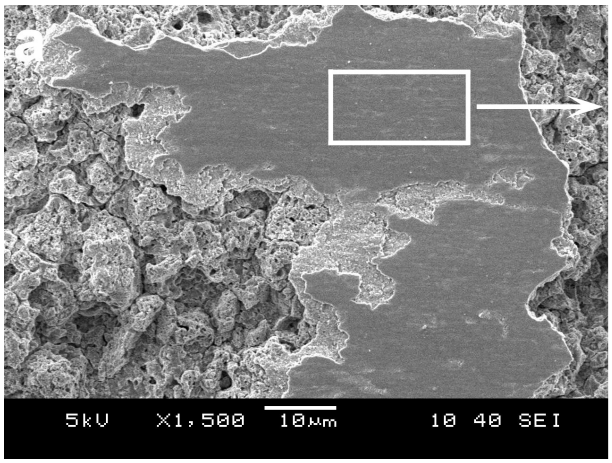


Figure 5.10 The optical microscope images of wear scar of counter body 100Cr6 steel bearing ball



Elemental com. (% wt)

Mg	**20.34**
Al	**29.45**
Fe	**11.29**
O	**38.92**

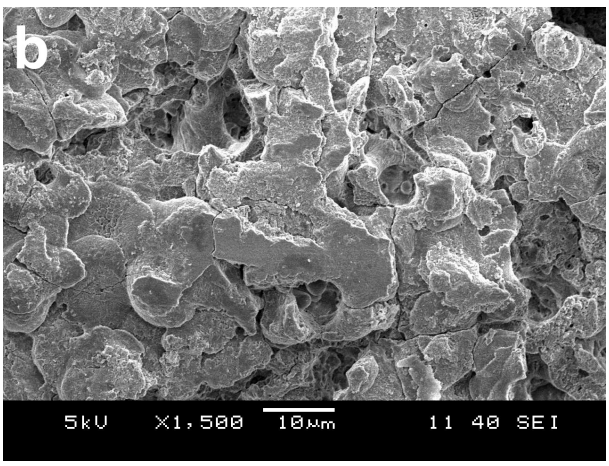


Figure 5.11 The SEM images taken from the wear track of (a) K10 and (b) K25 MAO coatings on AZ91D magnesium alloy

The wear profiles of coatings and bare magnesium alloys are shown in Figure 5.12. In case of MAO coatings the surface roughness profile remains almost unchanged. While K10 MAO coatings both on AZ91D and AM60B alloys show inward bending in their wear tracks due to their lower load bearing capacities than thicker coatings, K25 coatings exhibit almost unchanged surface profile with only some valleys which can be due to the particle removal from the surface. For bare magnesium alloys, the wear profiles look similar to the circular geometry of steel ball and it is easy to say that the main wear loss is observed on magnesium alloy rather than steel ball.

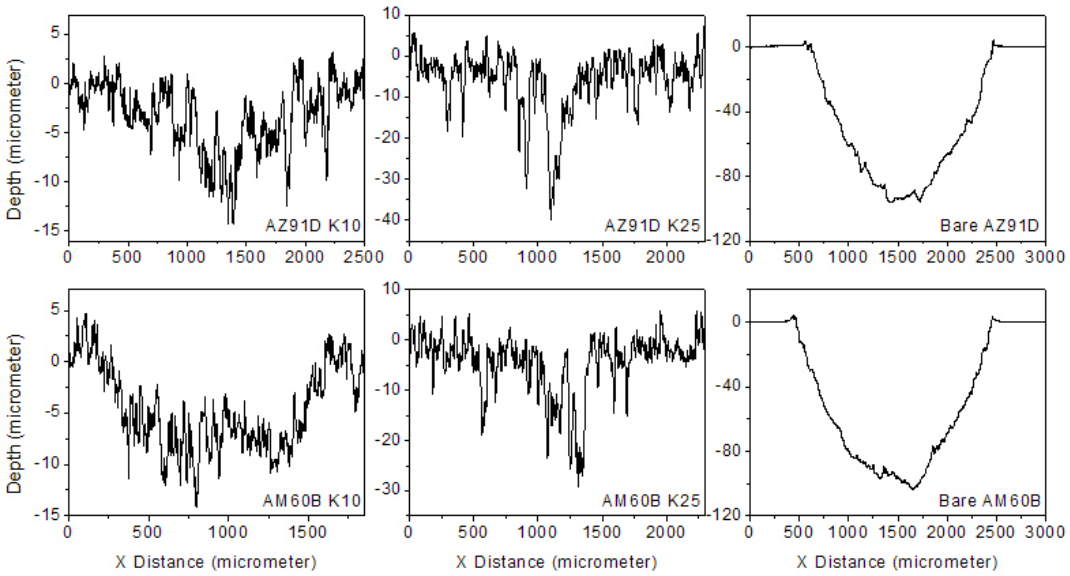


Figure 5.12 The wear scar profiles of coated and uncoated magnesium alloys

The wear losses of bare magnesium alloys and steel balls sliding against the MAO coatings are given in Table 5.3. While remarkable amount of material loss was observed for uncoated magnesium alloys, MAO coatings showed negligible coating removal appearing as surface flattening in SEM images (Figure 5.11) and the main volume loss was occurred on the steel ball in the wear tests of MAO coatings. Thus it is easy to say that the MAO coatings improved the wear resistance of magnesium alloys significantly. K25 MAO coatings exhibited greater wear resistance as compared to K10 coatings in terms of the increasing wear loss of steel ball. This is attributed to enhancing load bearing capacity of thicker coatings. However MAO

coatings on AZ91D alloy exhibited greater wear resistance due to their higher hardness value and adhesion strength as compared to AM60B alloy.

Table 5.3 The wear losses of uncoated magnesium alloys and steel balls slid against MAO coatings

Substrate	Wear loss (mm^3)		
	Bare magnesium alloy substrate*	K10 MAO coating**	K25 MAO coating**
AZ91D	1.153	-0.048	-0.088
AM60B	1.176	-0.041	-0.072

*The wear loss of bare magnesium alloy indicates the substrate volume loss

**The wear loss of MAO coatings reveals the volume loss of counter body (steel bearing ball)

CHAPTER SIX
CONCLUSIONS

6.1 General Results

In this study tribological properties of uncoated and MAO coated AZ91D and AM60B magnesium alloys were investigated using the scratch and dry sliding wear test methods. The following conclusions have been made;

1. As the duration of MAO process increased, the discharge events become more energetic and more violent. This leads to the formation of larger micropores with decreasing quantity. Thus, K25 MAO coatings showed higher surface roughness compared to K10 coatings. However, MAO coatings on AZ91D alloy showed smoother surface structure than AM60B alloy.

2. SEM images indicate that the coating is composed of two layers, a porous outer layer and a dense inner layer. Micropores are present merely in the porous outer layer, but they do not penetrate through the dense inner layer.

3. XRD analysis results indicate that MAO coatings are composed of MgO as main phase and other phases such as $AlPO_4$, $MgAlPO_5$ and $MgAl_2O_4$. Periclase (MgO) was formed via substrate metal oxidation during MAO treatment while $AlPO_4$ and $MgAlPO_5$ phases resulted from the contribution of alkaline electrolyte components into the coating structure.

4. The adhesion strength of MAO coatings were improved with increasing coating thickness. This may be the attributes of a denser film structure as well as the contributions of the MAO process which is expected to affect both the coating/substrate interface as well as the coating particles interface during subsequent dielectric breakdown and fusion events that occur as the coating thickness increases.

5. K10 and K25 MAO coatings on AZ91D and AM60B magnesium alloys revealed good wear resistance without any excessive wear damage. With increasing coating thickness, the wear resistance of MAO coatings improved due to increasing load bearing capacities. This result is in conjunction with the wear loss of steel bearing ball.

6. For uncoated magnesium alloys, abrasive and adhesive wear mechanisms acted together during sliding motion while abrasive wear mechanism was predominant for MAO coatings.

6.2 Future Plans

It is recommended that a further study should be carried out to obtain thicker coatings. With this aim, new coating electrolytes can be prepared and process parameters such as current density and its regime can be changed. In order to decrease the surface roughness, the outer porous layer of MAO coating can be removed by mechanical techniques, e.g. grinding, or can be sealed by further treatments, e.g. alkaline treatment in electrolyte. Also different electrolyte additives such as vanadates, molybdates and tungstates can be used to modify the mechanical properties of coatings. This can be beneficial for increasing the coating hardness which effects the tribological performance of coatings directly. However, different topcoats such as powder-coat, e-coat and Teflon can be applied on coatings to improve the wear resistance of coatings. These topcoats can exhibit finer surface structure and lower friction coefficient than MAO coatings. Lastly, the effect of oil lubrication on the tribological behaviour of MAO coatings can be studied.

REFERENCES

Albella, J. M., Montero, I., & Martinez-Duart, J. M. (1987). A theory of avalanche breakdown during anodic oxidation. *Electrochimica Acta, 32* (2), 255-258.

Anonymous. (1957). The HAE Process. *Light Metal Age, 15*, 10-14.

Arrabal, R., Matykina, E., Hashimoto, T., Skeldon, P., & Thompson, G. E. (2009). Characterization of AC PEO coatings on magnesium alloys. *Surface and Coatings Technology, 203,* 2207-2220.

ASTM G133 (2005). *Standard Test Method for Linearly Reciprocating Ball-on-Flat Sliding Wear*

Barton, T.F. (1998). *Anodization of magnesium and magnesium based alloys.* US Patent 5792335, USA.

Beauvir, J. (2004). *Oxidizing electrolytic method for obtaining a ceramic coating at the surface of a metal.* US Patent 6808613, USA.

Blau, P. J., & Walukas, M. (2000). Sliding friction and wear of magnesium alloy AZ91D produced by two different methods. *Tribology International, 33,* 573-579.

Blawert, C., Dietzel, W., Ghali, E., & Song, G. (2006). Anodizing Treatments for Magnesium Alloys and Their Effect on Corrosion Resistance in Various Environments. *Advanced Engineering Materials, 8* (6), 511-533.

Bunshah, R. (2001). *Handbook of Hard Coatings*. New York: William Andrew Publishing.

Cai, Q., Wang, L., Wei, B., & Liu, Q. (2006). Electrochemical performance of microarc oxidation films formed on AZ91D magnesium alloy in silicate and phosphate electrolytes. *Surface and Coatings Technology, 200* (12-13), 3727-3733.

Dahm, K. L., Black, A. J., Shrestha, S., & Dearnley, P. A. (2009). "*Plasma Electrolytic Oxidation treatment of aluminium alloys for lightweight disc brake rotors*", Proc. of Braking 2009: Institution of Mechanical Engineers (IMechE) conference June 2009, ISBN 1 84334 559 5.

Das, S. (2003). Magnesium for automotive applications: Primary production cost assessment. *Journal of the Minerals, Metals and Materials Society, 55* (11), 22-26.

Dearnley, P. A., Gummersbach, J., Weiss, H., Ogwu, A. A., & Davies, T. J. (1999). The sliding wear resistance and frictional characteristics of surface modified aluminium alloys under extreme pressure. *Wear, 225-229*, 127-134.

Duan, H., Yan, C., & Wang, F. (2007). Effect of electrolyte additives on performance of plasma electrolytic oxidation films formed on magnesium alloy AZ91D. *Electrochimica Acta, 52* (11), 3785-3793.

Duan, H., Yan, C., & Wang, F. (2007). Growth process of plasma electrolytic oxidation films formed on magnesium alloy AZ91D in silicate solution. *Electrochimica Acta, 52*, 5002–5009.

Evangelides, H. A. (1951). A new finish for magnesium alloys. *Metal Finishing, 55*, 56-60.

Evangelides, H. A. (1955). *Method of electrolytically coating magnesium and electrolyte therfor*. US Patent 2723952, USA.

Fontana, M. G. (1996). *Corrosion Engineering* (3rd ed.). USA: McGraw-Hill International Editions.

Gadow, R., Scherer, D. (2002). Composite coatings with dry lubrication ability on light metal substrates. *Surface and Coatings Technology, 151-152*, 471-477.

Gonzalez-Nunez, M. A., Nunez-Lopez, C. A., Skeldon, P., Thompson, G. E., Karimzadeh, H., Lyon, P., et al. (1995). A non-chromate conversion coating for magnesium alloys and magnesium-based metal matrix composites. *Corrosion Science, 37* (11), 1763-1772.

Gray, J. E., & Luan B. (2002). Protective coatings on magnesium and its alloys - a critical review. *Journal of Alloys and Compounds, 336* (1-2), 88-113.

Guo, J., Wang, L., Liang, J., Xue, Q., & Yan, F. (2009). Tribological behavior of plasma electrolytic oxidation coating on magnesium alloy with oil lubrication at elevated temperatures. *Journal of Alloys and Compounds, 481,* 903-909.

Hickling, A., & Ingram, M. D. (1964). Contact glow-discharge electrolysis. *Transactions of the Faraday Society, 60,* 783-793.

Hillis, J.E. (1994). Surface Engineering of Magnesium Alloys. In ASM Handbook, Surface Engineering Volume:5, ASM International.

Hoche, H., Blawert, C., Broszeit, E., Berger, C. (2004). "Corrosion Properties of PVD-coated Magnesium Die Cast Alloy AZ91D Part I: Investigation of the Corrosion Properties and the Corrosion Mechanisms of PVD Coated Magnesium Die Cast Alloy AZ91 for Tribological Applications" In: K.U. Kainer, Editor, *Proceedings of the 6th International Conference Magnesium Alloy and Their Applications*, Wiley, pp. 559-567.

Hoche, H., Scheerer, H., Probst, D., Broszeit, E., & Berger, C. (2003). Development of a plasma surface treatment for magnesium alloys to ensure sufficient wear and corrosion resistance. *Surface and Coatings Technology, 174-175*, 1018-1023.

Hoche, H., Schroeder, H. J., Scheerer, H., Broszeit, E., & Berger, C. (2002). Tribological Studies of CrN coated Magnesium AZ91 at Temperatures up to 250°C. *Advanced Engineering Materials, 4* (1-2), 42-51.

Hollstein, F., Wiedemann, R., & Scholz, J. (2003). Characteristics of PVD-coatings on AZ31hp magnesium alloys. *Surface and Coatings Technology, 162* (2-3), 261-268.

Hsiao H., & Tsai, W. (2005). Characterization of anodic films formed on the AZ91D magnesium alloy. *Surface and Coating Technology, 190*, 299-308.

Huber, K. (1953). Anodic Formation of Coatings on Magnesium, Zinc, and Cadmium. *Journal of The Electrochemical Society, 100* (8), 376-382.

Hutchins, S., Shashkov, P., Samsonov, V., & Shatrov, A. (2004). "New Generation of Keronite Process for Corrosion Protection of Magnesium" In: K.U. Kainer, Editor, *Proceedings of the 6th International Conference Magnesium Alloy and Their Applications*, Wiley, pp. 553-558.

Hutchins, S., Shrestha, S., Sturgeon, A., Shashkov, P., & Shatrov, A. (2004). "The Corrosion Performance of Sealed KERONITE Coatings on AZ91D Magnesium Alloy" In: K.U. Kainer, Editor, *Proceedings of the 6th International Conference Magnesium Alloy and Their Applications*, Wiley, pp. 617-622.

Ikonopisov, S., Girginov, A., & Machkova, M. (1979). Electrical breaking down of barrier anodic films during their formation. *Electrochimica Acta, 24* (4), 451-456.

Jin, F., Chu, P. K., Xu, G., Zhao, J., Tang, D., & Tong, H. (2006). Structure and mechanical properties of magnesium alloy treated by micro-arc discharge oxidation using direct current and high-frequency bipolar pulsing modes. *Materials Science and Engineering: A, 435-436,* 123-126.

Kainer, K. U. (2003). Magnesium Corrosion-Processes, Protection of Anode and Cathode. In *Magnesium Alloys and Technology* (230-231). Germany: Wiley-VCH.

Klapkiv, M. D. (1995). State of an electrolytic plasma in the process of synthesis of oxides based on aluminum. *Materials Science, 31* (4), 494-499.

Klein, N. (1978). Electrical breakdown mechanisms in thin insulators. *Thin Solid Films, 50,* 223-232.

Krishna, L. R., Purnima, A. S., & Sundararajan, G. (2006). A comparative study of tribological behavior of microarc oxidation and hard-anodized coatings. *Wear, 261,* 1095-1101.

Liang, J., Guo, B., Tian, J., Liu, H., Zhou, J., & Xu T. (2005). Effect of potassium fluoride in electrolytic solution on the structure and properties of microarc oxidation coatingson magnesium alloy. *Applied Surface Science*, *252* (2), 345-351.

Liang, J., Hu, L., & Hao, J. (2007). Improvement of corrosion properties of microarc oxidation coating on magnesium alloy by optimizing current density parameters. *Applied Surface Science, 253* (16), 6939-6945.

Liang, J., Wang, P., Hu, L., & Hao, J. (2007). Tribological properties of duplex MAO/DLC coatings on magnesium alloy using combined microarc oxidation and filtered cathodic arc deposition. *Materials Science and Engineering: A*, *454-455*, 164-169.

Lugscheider, E., Parco, M., Kainer, K. U., & Hort, N. (2004). "Thermal Spraying of Magnesium Alloys for Corrosion and Wear Protection" In: K.U. Kainer, Editor, *Proceedings of the 6th International Conference Magnesium Alloy and Their Applications*, Wiley, pp. 860-868.

Lunder, O., Lein, J. E., Aune, T. K., & Nisancioglu, K. (1989). The Role of $Mg_{17}Al_{12}$ Phase in the Corrosion of Mg Alloy AZ91. *Corrosion, 45*, 741-748.

McNeill, W., & Gruss, L. L. (1966). *Anodic spark reaction processes and articles*. US Patent 3293158, USA.

McNeill, W., & Nordbloom, G. F. (1958). *Method of making cadmium niobate*. US Patent 2854390, USA.

Merstallinger, A., Semerad, E., & Dunn, B. D. (2003). "*Influence of coatings and Alloying on Cold Welding due to Impact and Fretting*", Proc. 9th European Space Symposium on Material in a Space Environment, ESTEC Noordwijk (NL).

Miao, Q., Cui, C. E., & Pan, J. D. (2007). CrN–TiN multilayer coating on magnesium alloy AZ91 by arc-glow plasma depositing process. *Surface and Coatings Technology, 201* (9-11), 5077-5080.

Mistry, K., Priest, M., & Shrestha, S. (2008). "*The potential of plasma electrolytic oxidised eutectic Al-Si alloy as a cylinder wall surface for lightweight engine blocks*", IMechE Proceedings, Tribology 2008: Surface engineering of automotive powertrains for environmentally friendly transport.

Mittal, C.K. (1995). Transactions of the Metal Finishers Association. *Metal Finishing, 91* (4), 227.

Nie, X., Leyland, A., Song, H. W., Yerokhin, A. L., Dowey, S. J., & Matthews, A. (1999). Thickness effects on the mechanical properties of micro-arc discharge oxide coatings on aluminium alloys. *Surface and Coatings Technology, 116-119,* 1055-1060.

Nie, X., Meletis, E. I., Jiang, J. C., Leyland, A., Yerokhin, A. L., & Matthews, A. (2002). Abrasive wear/corrosion properties and TEM analysis of Al_2O_3 coatings fabricated using plasma electrolysis. *Surface and Coatings Technology, 149,* 245-251.

Rakoch, A. G., Khokhlov, V. V., Bautin, V. A., Lebedeva, N. A., Magurova, Y. V., Bardin, I. V. (2006). Model concepts on the mechanism of microarc oxidation of metal materials and the control over this process. *Protection of Metals, 42* (2), 158-169.

Rao, V. D. N., Cikanek, H. A., Boyer, B. A., Lesnevsky, L. N., Tchernovsky, N. M., & Tjurin, N. V. (1997), Friction and wear characteristics of micro-arc oxidation coating for light weight, wear resistant, powertrain component application, *SAE Technical Paper Series* 970022.

Shimadzu Co. (2003). Scanning Scratch Tester SST-W101 Instruction Manual (2003) p. 4-5

Snizhko, L. O., Yerokhin, A. L., Pilkington, A., Gurevina, N. L., Misnyankin, D. O., Leyland, A., & Matthews A. (2004). Anodic processes in plasma electrolytic oxidation of aluminium in alkaline solutions. *Electrochimica Acta*, *49* (13), 2085-2095.

Srinivasan, P. B., Blawert, C., & Dietzel, W. (2009). Dry sliding wear behaviour of plasma electrolytic oxidation coated AZ91 cast magnesium alloy. *Wear, 266,* 1241-1247.

Sundararajan, G., & Krishna, L. R. (2003). Mechanisms underlying the formation of thick alumina coatings through the MAO coating technology. *Surface and Coatings Technology*, *167* (2-3), 269-277.

Udhayan, R., & Bhatt D. P. (1996). On the corrosion behaviour of magnesium and its alloys using electrochemical techniques. *Journal of Power Sources, 63* (1), 103-107.

Umehara, H., Takayaand, M., & Terauchi, S. (2003). Chrome-free surface treatments for magnesium alloy. *Surface and Coatings Technology,169-170,* 666-669.

Unger, R.H. (1987). "Thermal spray coatings". In *ASM Handbook Corrosion Volume 13*. (459). USA: ASM International.

Van, T. B., Brown, S. D., & Wirtz, G. P. (1977). Mechanism of Anodic Spark Deposition. *A.C.S. Bulletin, 56* (6), 563-566.

Wagner, H. E., Brandenburg, R., Kozlov, K. V., Sonnenfeld, A., Michel, P., & Behnke, J. F. (2003). The barrier discharge: basic properties and applications to surface treatment. *Vacuum*, *71* (3), 417-436.

Ximei, W., Liqun, Z., Huicong, L., & Weiping, L. (2008). Influence of surface pretreatment on the anodizing film of Mg alloy and the mechanism of the ultrasound during the pretreatment. *Surface and Coatings Technology, 202* (17), 4210-4217.

Yamauchi, N., Demizu, K., Ueda, N., Cuong, N. K., Sone, T., & Hirose Y. (2005). Friction and wear of DLC films on magnesium alloy. *Surface and Coatings Technology, 193* (1-3), 277-282.

Yerokhin, A. L., Leyland, A., & Matthews, A. (2002). Kinetic aspects of aluminium titanate layer formation on titanium alloys by plasma electrolytic oxidation. *Applied Surface Science, 200* (1-4), 172-184.

Yerokhin, A. L., Lyubimov, V. V., & Ashitkov, R. V. (1998). Phase formation in ceramic coatings during plasma electrolytic oxidation of aluminium alloys. *Ceramics International*, *24* (1), 1-6.

Yerokhin, A.L., Nie, X., Leyland, A., & Matthews, A. (2000). Characterisation of Oxide Films produced by Plasma Electrolytic Oxidation of a Ti-6Al-4V alloy. *Surface and Coatings Technology, 130* (2-3), 195-206.

Yerokhin, A. L., Nie, X., Leyland, A., Matthews, A., Dowey S. J. (1999). Plasma electrolysis for surface engineering. *Surface and Coatings Technology, 122* (2-3), 73-93.

Yerokhin, A. L., Shatrov, A., Samsonov, V., Shashkov, P., Leyland, A., & Matthews, A. (2004). Fatigue properties of Keronite® coatings on a magnesium alloy. *Surface and Coatings Technology, 182* (1), 78-84.

Yerokhin, A. L., Snizhko, L. O., Gurevina, N. L., Leyland, A., Pilkington, A., & Matthews, A. (2003). Discharge characterization in plasma electrolytic oxidation of aluminium. *Journal of Physics D: Applied Physics, 36* (17), 2110-2120.

Yerokhin, A. L., Snizhko, L. O., Gurevina, N. L., Leyland, A., Pilkington, A., & Matthews, A. (2004). Spatial characteristics of discharge phenomena in plasma electrolytic oxidation of aluminium alloy. *Surface and Coatings Technology, 177-178*, 779-783.